water

MDPI

Article

Projection of Climate Change and Consumptive Demands Projections Impacts on Hydropower Generation in the São Francisco River Basin, Brazil

Marx Vinicius Maciel da Silva [1,*], Cleiton da Silva Silveira [1], José Micael Ferreira da Costa [2], Eduardo Sávio Passos Rodrigues Martins [1,3] and Francisco das Chagas Vasconcelos Júnior [3]

[1] Hydraulic and Environmental Engineering Department (DEHA), Federal University of Ceará (UFC), Fortaleza-CE 60455-760, Brazil; cleitonsilveira@ufc.br (C.d.S.S.); espr.martins@gmail.com (E.S.P.R.M.)
[2] Higher Engineering Institute of Porto (ISEP), 4200-072 Porto, Portugal; jmicaelcosta@gmail.com
[3] Research Institute for Meteorology and Water Resources (FUNCEME), Fortaleza-CE 60115-221, Brazil; francisco.vasconcelos@funceme.br
* Correspondence: marx.silva@alu.ufc.br

Abstract: Climate change impacts may influence hydropower generation, especially with the intensification of extreme events and growing demand. In this study, we analyzed future hydroelectric generation using a set of scenarios considering both climate change and consumptive demands in the São Francisco River Basin. This project will increase consumptive demands for the coming decades. Five models from the recently released Coupled Model Intercomparison Project Phase 6 and two scenarios, SSP2-4.5 and SSP5-8.5, were considered to estimate climate change projections. The affluent natural flows, regulated flows, and the hydroelectric energy generated were estimated for four multi-purpose reservoirs considering all existing and new demands. The conjunction of scenarios indicated a possible significant reduction in water availability, increased consumptive demands, especially for irrigation, and reduced power generation. Only at the Sobradinho hydroelectric plant, the decrease ranged from −30% to −50% for the period 2021 to 2050 compared to the historical period (1901 to 2000). The results can provide insights into future energy generation and water resources management in the basin.

Keywords: climate change; hydroelectric generation; conflicting demands; water resources management

Citation: da Silva, M.V.M.; Silveira, C.d.S.; Costa, J.M.F.d.; Martins, E.S.P.R.; Vasconcelos Júnior, F.d.C. Projection of Climate Change and Consumptive Demands Projections Impacts on Hydropower Generation in the São Francisco River Basin, Brazil. *Water* **2021**, *13*, 332. https://doi.org/10.3390/w13030332

Academic Editor: Shuo Wang
Received: 30 December 2020
Accepted: 25 January 2021
Published: 29 January 2021

1. Introduction

Extreme events such as severe droughts have increased globally in recent years [1]. Such events significantly influence several sectors such as energy production, agriculture, the economy, and society. Hydropower generation is the most widely used renewable energy resource in the world [2]. Its production is highly connected with the consumptive demands for food production and municipal water supply. With growing demands and modification of the current climate, increasing pressure may arise in hydropower generation and cause important changes in water management, particularly during the occurrence of prolonged droughts.

The Northeast Brazil Region (NBR) suffers from recurrent prolonged droughts, directly affecting this region's water, food, and energy security. Since the 18th century, eight drought events persisted for more than three years [3]. However, the recent multiannual drought of 2012–2018 (seven years) was the most prolonged and severe one [3,4]. Due to this historical coexistence with droughts, both National and State Governments have taken measures to mitigate the impact of these events with the construction of multiyear reservoirs, and lately, cisterns, canals, and social programs to assist the most vulnerable populations [5].

The São Francisco River hydroelectric system produces most of the electric power consumed by the NBR. The basin can generate 16,551 GWh per year, 12% of the nation's

total electricity production [6]. However, conflicting uses also exist, especially with growing demands for agriculture and the city's water supply.

In addition to current demands, a water transfer project from the São Francisco River to the semi-arid Northeast of Brazil is being concluded to reduce vulnerability to droughts and promote regional development. This extra demand will provide water for various purposes, such as human, animal, and irrigation, and fish and shrimp farming, in an area of about 12 million inhabitants [7]. However, this new demand will enhance existing water conflicts, especially during extreme events such as the 2012–2018 drought, when water supply to urban areas was prioritized, in accordance to the federal water resources law, as well as food production rather than electricity generation [8].

The NBR experienced a drastic reduction in the total energy demand supplied by hydroelectric energy during the recent drought. In November 2015 and 2017, the water volume level in the São Francisco River reservoirs dropped to only 5% of the total capacity in terms of stored energy. This level was the lowest since all dams were completed in 1994 [6]. The decline in hydroelectricity generation is being replaced mainly by fossil fuel energy, as it was the case in 2014, with a 47% share in the total electricity generated for the region [9]. This type of electricity generation emits carbon dioxide (CO_2) into the atmosphere, acting as positive feedback for climate change since it intensifies the greenhouse effect. In this context, the concept of climate, water, energy, and food nexus has become increasingly important in assessing the possible long-term impacts on various sectors of society and, with this, helping with the planning of water and energy resources and mitigation strategies for the possible impacts on these sectors. In addition, hydropower production, often considered a clean and renewable energy source and environmentally better compared to fossil fuels, can also bring environmental damage to ecosystems. For in this type of generation, river flows are altered through dams, which can alter or diminish the ecosystems and biodiversity of a region [10]. Therefore, the increase in demand for electricity also generates a tension between the goals related to reducing CO_2 emissions and those related to ecosystem conservation, through the trade-off between protected areas and the expansion of hydroelectric plants. Several studies have shown that it is necessary to compromise the production of energy from hydroelectric plants in order to improve environmental protection in several regions of the world [10–13]. Thus, besides the climate, water, and energy nexus, the water, energy, and ecosystem nexus is also known.

In order to assess the impacts associated with climate change, the Intergovernmental Panel on Climate Change (IPCC) was established by the United Nations Environment Programme (UNEP) and the World Meteorological Organization (WMO) in 1988 [1]. Since its creation, the IPCC has been releasing Assessment Reports (AR) on climate change, releasing several projection scenarios using different Global Climate Models (GCM—General Circulation Model) based on the emission of Greenhouse Gases [1].

These models follow standardization among the various Institutes that cooperate in the project, called the Intercomparison Model Projects (CMIP), linked to the World Climate Research Programme (WCRP) and is in its fifth phase (CMIP5). Several studies using IPCC models in its fifth phase (CMIP5) showed that the average annual rainfall in the NBR could decrease by approximately 25% to 50% depending on the emissions scenario for the 21st century when compared to the 20th century [14–17]. Precipitation anomalies between −20% and 20% were shown by [17] for the São Francisco River basin every 30 years (2011 to 2040, 2041 to 2070, and 2071 to 2100). According to [8], after analyzing a 57-year rainfall time series, they found that the rainfall already shows a decline of more than 25% from the historical average of 1961 to 1990, being below its average since 1992. Thus, the authors of [8] say that if this declining trend continues, the reduction in rainfall in this basin may be even more severe than the projections of the more pessimistic models.

Besides the possible decrease in the average annual precipitation in the NBR, these works also showed an increase in temperature of approximately 4° to 5 °C [14–17]. Higher temperatures and significantly reduced rainfall may result in reductions in the rates of

affluent natural flows ranging from 60% to 90% for the 21st century compared to the 20th century for various river basins in the NBR [18,19].

The sixth phase of the CMIP project (CMIP6) has recently started to release the first results of the models. It brings advances in CGMs modeling and future scenario considerations [20]. The combination of socio-economic and technological development with future radiative forcing scenarios based on updated data on emissions trends was the innovation of CMIP6 climate projections compared to CMIP5 [20,21].

Although several climate change impacts on the São Francisco River Basin have been reported, the impacts on hydroelectricity generation due to future climate associated with growing consumptive uses are rarely addressed, especially using the most recent CMIP6 models. The increase in water demand for the coming decades, caused by population and wealth growth, enhanced agricultural demand due to higher temperatures and the addition of new demands by a water transfer project may exert significant pressure on the hydroelectric power generation of the NBR [16,18].

To confirm this assumption, we proposed a set of scenarios to consider both climate changes and consumptive demand growth. We evaluated how each demand can increase, and its impact on hydroelectricity production using future affluent natural flows.

Thus, this paper aimed at clarifying the role of climate change and growing demands on hydroelectricity production by estimating the impacts that the future climate projected by the recent CMIP6 models and combined with the growth of projected consumptive demands may cause on the affluent natural flows and hydroelectric power generation on the São Francisco River basin. Results should help decision-makers to better prepare for future scenarios and to reduce climate change impacts on the water–energy–food nexus.

2. Materials and Methods

The responses of the affluent natural flows and hydroelectric generation were analyzed based on the future climate scenarios SSP2-4.5 and SSP5-8.5 of the CMIP6 models and the possible future scenarios of consumptive demands. The affluent natural flows and future demands for each basin of the reservoir, followed by hydroelectric production for these scenarios were estimated, a process divided into six stages, according to Figure 1.

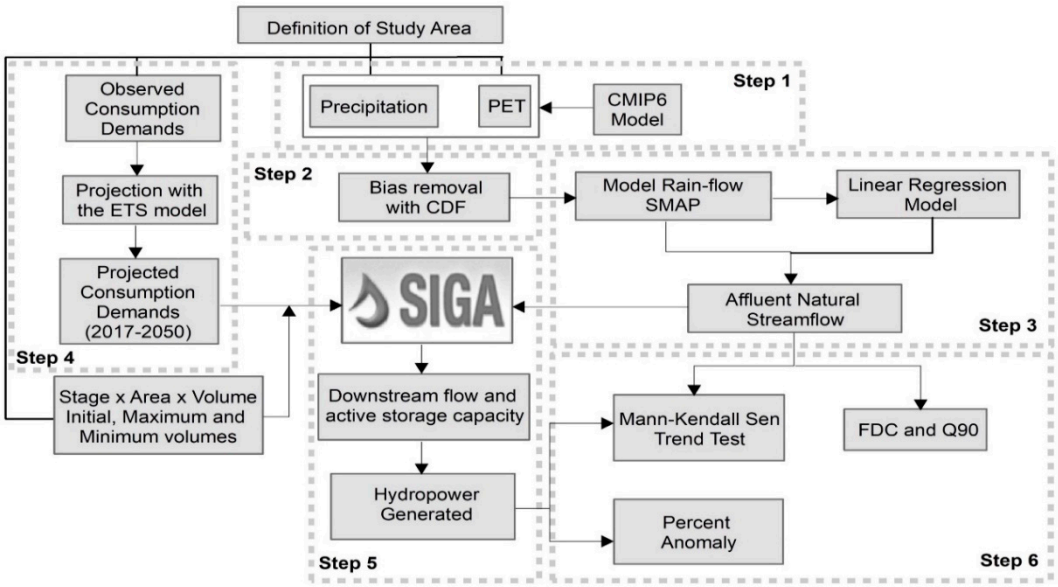

Figure 1. Flowchart of the methodological stages.

In Step 1, the annual time series of precipitation variables and maximum, minimum and mean upper air temperatures (UAT) observed, as well as those projected by CMIP6 were extracted with the classic Thiessen method [22] for the basin of the reservoirs of São

Francisco River Basin (SFRB). Still in Step 1, potential evapotranspiration was estimated with the maximum, minimum, and mean UAT using the Hargreaves–Sammani method.

In Step 2, the statistical corrections to remove bias from the precipitation and Potential Evapotranspiration (PET) time series of the CMIP6 models were performed with the observed data. For this purpose, the gamma cumulative distribution function (CDF) was used.

In Step 3, the precipitation and PET data with bias removed from the CMIP6 were used as input by the hydrological rainfall-runoff model soil moisture accounting procedure (SMAP) to generate the natural flow data from the basins of Retiro Baixo, Sobradinho, Itaparica, and Três Marias. Still in Step 3, the affluent natural flows were estimated for the remaining reservoirs (Xingó, Moxotó, Complexo Paulo Afonso and Queimado). For this purpose, we used the natural flow data generated with the SMAP model and the monthly series of naturalized flows made available by the Brazilian National Electrical System Operator (ONS in Portuguese), dividing them in two groups with four reservoirs each. The four reservoirs with the calibrated SMAP model were used to predict the affluent natural flows for the other four remaining reservoirs.

In Step 4, the municipal demands were quantified with geoprocessing techniques and aggregated for each main reservoir. Then, their projections for the period 2017 to 2050 were estimated using the exponential smoothing model.

In Step 5, the operation of the reservoir was simulated, focusing on meeting water demands through the Information System for Water Allocation Management (SIGA in Portuguese) software [23]. For this purpose, the natural flow data obtained with the SMAP model, data from the CMIP6 models in the SSP2-4.5 and SSP5-8.5 scenarios, and the consumptive demands scenarios were used. Still in Step 5, with the SIGA simulation results, it was possible to estimate the hydroelectric energy generation.

In Step 6, the regularized flows with 90% duration (Q90) and hydroelectric power analysis were performed through the Mann–Kendall Sen test and percentage anomaly. The next topics discuss the study region, database, and methodology applied.

2.1. Study Area

The study region of this work was the SFRB, as shown in Figure 2. It drains an area of 639,219 km^2, which is equivalent to about 8% of the Brazilian territory. Starting in Serra da Canastra in Minas Gerais, the São Francisco River is 2700 km long. It flows through the states of Bahia and Pernambuco in a south-north direction, reaching the Atlantic Ocean through the border of Alagoas and Sergipe. SFRB traverses seven states: Bahia, Minas Gerais, Pernambuco, Alagoas, Sergipe, Goiás, and Distrito Federal. Besides, it covers 507 municipalities (almost 9% of all municipalities in Brazil), with a resident population that reaches 20 million people [24].

The main SFRB reservoirs are Três Marias, Sobradinho, and Itaparica (also known as Luíz Gonzaga), which have useful volumes of 15,278 hm^3, 28,669 hm^3 and 3549 hm^3, and surface areas of 1040 km^2, 4214 km^2 and 828 km^2, respectively [25]. The water transfer project will divert water in the São Francisco River between Sobradinho and Itaparica dams, in the State of Pernambuco (see Figure 2). The project comprises two independent canals, water pumping stations, small reservoirs, and a hydroelectric power plant (HPP). It will meet the water supply needs for multiple uses in the states of Pernambuco, Paraíba, Rio Grande do Norte, and Ceará [24].

The project region is known for long periods of drought. The area that suffers the most from the effects of these prolonged droughts is located in the semi-arid part north of the São Francisco River. This area partially covers the states of Pernambuco, Ceará, Paraíba, and Rio Grande do Norte (regions that will be comprised with the transposition). The enterprise will enable water supply for various purposes (human, irrigation, and animal supply, fish, and shrimp farming) in an area with about 12 million inhabitants [24]. Before completing the transposition axes, the current total demand in the basin accounts for 77% of irrigation, 11% of urban demand, and 7% of industrial demand [24].

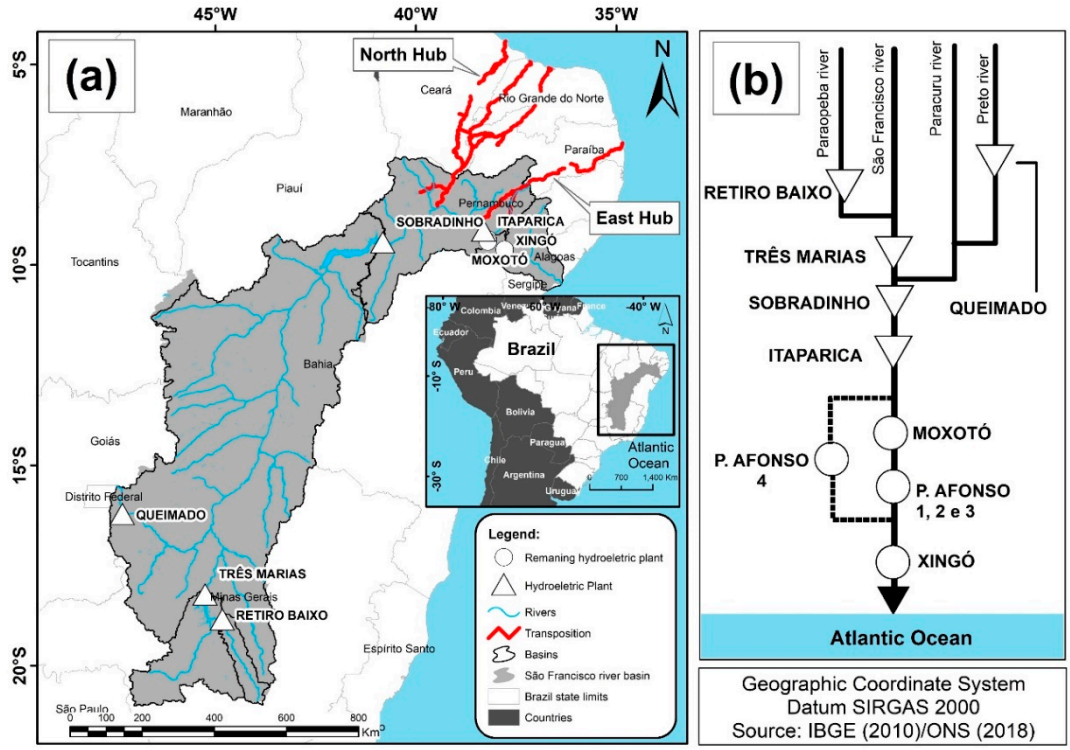

Figure 2. Location of Reservoirs, the water transfer canals in the Northeast Brazil Region (NBR) in (**a**), and schematic diagram of the hydroelectric power plant (HPP) belonging to the (**b**).

Besides meeting the consumptive demands, SFRB plays an essential role in electricity generation, with installed potential corresponding to 12% of the nation's total [25]. However, due to the drought in the region that began in 2012, hydroelectric generation supplied only 56%, 42%, 34%, 30%, 21%, and 21% of the total electrical energy demand by the NBR from 2013 to 2018. This production was far below previous years. The decline in hydroelectricity production is illustrated in Figure 3. This shortfall was mainly replaced by fossil fuel energy (thermal) with 39%, 47%, 42%, 33% and 25%, and the growth of wind energy with an increase from 5% to 52% during this period.

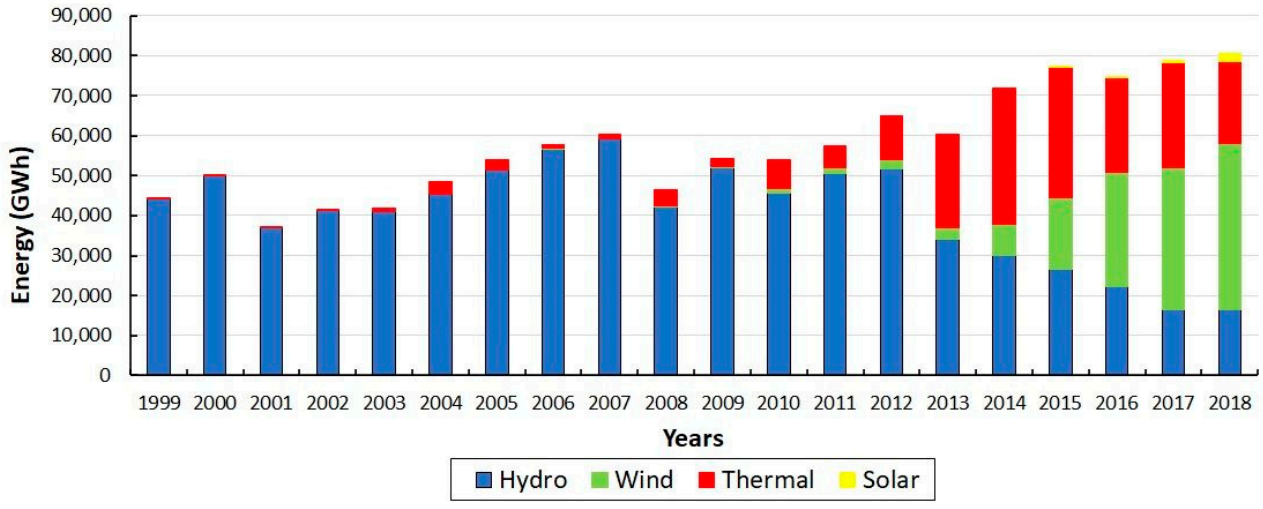

Figure 3. Generation of electric energy by type for the NBR. Data Source: [9].

2.2. Observed Data

For the calibration of the parameters of the SMAP rainfall-runoff model, monthly historical precipitation data obtained from the Brazilian National Water Agency (in Portuguese, ANA) rainfall stations from 1961 to 2016 [26] and maximum, minimum, and mean temperatures from the Climate Research Unit (CRU) with spatial resolution of 0.5° × 0.5° were used [27]. General information on the Level-Area-Volume curve of the reservoirs for the SIGA program usage was obtained from the operating reservoir companies, the Minas Gerais Energy Company (CEMIG) regarding the Três Marias reservoir, and the São Francisco Hydroelectric Company (CHESF) for the other reservoirs [25,28]. Finally, the monthly hydroelectric energy observed from 1999 to 2016 from the HPP of the São Francisco River was obtained from the ONS and used to validate the hydroelectric energy simulated by the SIGA software [9].

2.3. Coupled Model Intercomparison Project Phase 6

Recently, updated data from the GCM regarding the sixth phase of CMIP, CMIP6, were made available. The data from CMIP6 are the results of the simulations of five GCMs: Canadian Earth System Model 5nd generation (CanESM5), Institut Pierre-Simon Laplace—5 Component Models version A—Medium Resolution (IPSL-CM5A-MR), Model for Interdisciplinary Research on Climate version 6 (MIROC6), Beijing Climate Center—Climate System Model version 2—Medium Resolution (BCC-CSM2-MR), and Meteorological Research Institute Earth System Model Version 2.0 (MRI-ESM2.0), according to Table 1.

Table 1. CMIP6 (Intercomparison Model Projects) models: the 5 General Circulation Models (GCMs) used in this study.

Models	Institute (Country)	Resolution	Citations
CanESM5	Canadian Earth System Model 5nd generation (Victoria, BC, Canada)	1° × 1°	[29]
IPSL-CM5A-MR	Institut Pierre-Simon Laplace (Paris, France)	1.25° × 1.25°	[30]
MIROC6	Atmosphere and Ocean Research Institute, National Institute for Environmental Studies, and Japan Agency for Marine-Earth Science and Technology (Tokyo, Japan)	1.4° × 1.4°	[31]
BCC-CSM2-MR	Beijing Climate Center climate system model version 2 (Beijing, China)	1° × 1°	[32]
MRI-ESM2.0	Meteorological Research Institute of the Japan Meteorological Agency (Tokyo, Japan)	1° × 1°	[33]

In this study, the precipitation variables, monthly mean, maximum and minimum UAT for the historical scenario (1901 to 2000, 20th century) and SSP2-4.5 and SSP5-8.5 projection scenarios for the 21st century were used (2016–2100).

There are five different shared socioeconomic pathways (SSPs). The future sustainable potential and fossil fuel-driven growth are the most extreme scenarios, SSP1 and SSP5, respectively [34]; high inequality between or within countries, are given by SSP3 and SSP4, respectively [35] and the SSP2 scenario is the "middle term" of the aforementioned scenarios [36]. For each SSP, different Representative Concentration Pathways (RCPs) represent different radiative forcing projections leading to an extensive range of global warming levels throughout the century [37]. This new structure allows the standardization of all socio-economic assumptions (e.g., population, gross domestic product and poverty, among others) in each scenario's modeled representations. Plus, it allows a more subtle investigation of the variety of paths that climate outcomes can follow.

2.4. PET Estimation through Hargreaves–Samani Method

For PET estimation, the mean, maximum and minimum UAT data (in Celsius degrees) of the CMIP6 models were used in the SSP2-4.5 and SSP5-8.5 projection scenarios using the Hargreaves–Samani method [38,39], according to Equation (1):

$$\mathrm{PET} = 0.0023(\mathrm{UAT_{max}} - \mathrm{UAT_{min}})^{0.5}(\mathrm{UAT_{med}} + 17.8)\mathrm{Ra}, \quad (1)$$

where PET is given in mm/month; and the Average External Radiation (Ra) was estimated from the latitude and month of the year, according to the work of [38].

2.5. Bias Correction

The results of climate models, such as the CMIP6 models, show systematic errors, especially related to bias [40]. Thus, the statistical correction via CDF with the mapping probability was performed in a monthly time series of precipitation and PET to reduce such errors. CDF is widely used in several studies that use climate models, for bias correction of precipitation and PET variables [17–19,41].

The methodology is based on the study by [42] in which the accumulated probability distribution curves of the monthly modeled and observed series are generated, obtaining 12 gamma adjustments, one for each month of the year. After that, it was possible to check the probabilistic behavior of the modeled data in relation to those observed. Thus, the corrected precipitation/PET value of the CMIP6 models was obtained by taking the precipitation/PET value corresponding to the same probability of occurrence in the observed values curve.

2.6. The Soil Moisture Accounting Procedure (SMAP) Rainfall-Runoff Hydrological Model

In this study, the monthly SMAP model was used. Developed by [43], it uses little observational data and low computational demands, making it very popular. SMAP covers the process of hydrological balance in two hypothetical reservoirs, one of soil (R_{soil}) and one underground (R_{sub}).

The water stored in each reservoir is updated at each time interval due to the incorporation of a new average rainfall data through the following transfer Equations (2)–(5):

$$E_s = T_u{}^{P_{es}} \cdot P, \quad (2)$$

$$E_r = T_u \cdot E_p, \quad (3)$$

$$R_{ec} = C_{rec} \cdot T_u{}^4 \cdot R_{soil}, \quad (4)$$

$$E_b = (1 - K) \cdot R_{sub}, \quad (5)$$

where E_s is the surface flow (mm), P is the precipitation (mm), T_u is the initial moisture content (adimensional), E_r is the actual evapotranspiration, E_p is the potential evapotranspiration (mm), P_{es} is the surface flow parameter (adimensional), C_{rec} is the recharge coefficient (adimensional), E_b is the base flow (mm), K the recession constant (month^{-1}), R_{soil} is the soil reservoir, R_{sub} is the underground reservoir and R_{ec} is the underground recharge. Figure 4 shows how the monthly SMAP model works.

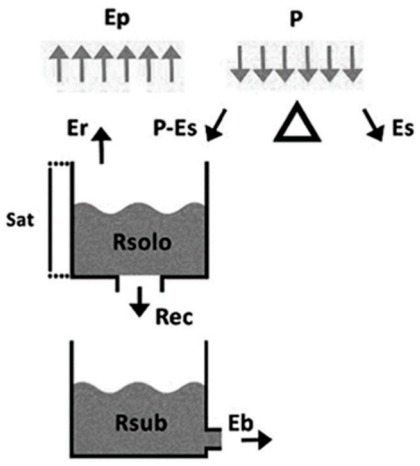

Figure 4. Schematic monthly soil moisture accounting procedure (SMAP) model. Source: [43].

T_{uin} is the initial soil moisture rate that determines the initial level of the second reservoir R_{soil} and the initial base flow (E_{bin}) that defines the initial value of R_{sub}. In this work, the calibration took place in a single step, in which the parameters Sat, P_{es} and C_{rec} and K of level R_{sub} that generates the E_b underwent an optimization through the solver tool present in the Microsoft Excel spreadsheet, followed by a manual refinement by trial and error. Additionally, T_{uin} and E_{bin} were manually adjusted with the Nash–Sutcliffe efficiency coefficient (NASH) for each simulation.

According to [44], NASH is one of the most used criteria in Hydrology and is an objective function that measures the adjustment efficiency between a model and observed data. According to the formulation presented by [45], NASH is calculated through Equation (6):

$$NASH = 1 - \frac{\sum_{i=1}^{N}(o_i - m_i)^2}{\sum_{i=1}^{N}(o_i - \overline{o_i})^2}, \quad (6)$$

where N the samples number, o_i the observed data, m_i the data being modeled and $\overline{o_i}$ the average of the observed data.

The reference values for NASH coefficient, suggested by [44,46], classify as acceptable the values from 0.36 to 0.75 and excellent above 0.8. Its maximum value corresponding to 1, which indicates a perfect adjustment between the modeled and observed data. Table 2 shows the parameters of the SMAP model calibrated for the SFRB reservoirs, using the estimated natural flow data from the ONS. The different periods in the calibration of the reservoirs took place according to the availability of data from ANA stations. From those, only the Itaparica reservoir was not classified as excellent calibration, presenting an acceptable NASH coefficient.

Table 2. Parameters and SMAP calibration for each simulated hydrosystems.

Reservoir	Area (km^2)	Calibration Period	NASH	T_{uin}	E_{bin}	Sat	P_{es}	C_{rec}	K
Retiro Baixo	12,187	07/1986–07/1993	0.86	68.66	54.74	3240.12	8.34	1.89	0.09
Três Marias	50,732	07/1971–07/1978	0.90	86.36	212.8	11,769.15	8.05	2.6	0.02
Sobradinho	467,000	07/1998–07/2005	0.90	60.7	751.6	1500.14	5.75	4.10	0.01
Itaparica	593,400	07/1983–07/1990	0.36	97	760	7977	5.6	0.69	13.25

2.7. Linear Regression Model

The linear regression model was used in this study to generate the flow rates of the HPP that do not have the calibrated SMAP model (Queimado, Xingó, Moxotó, Complexo Paulo Afonso 1, 2, 3 and 4). This model was used with good performance at representing the flows in several reservoirs [17,19]. The first methodological stage occurred with the standardization of the monthly series of naturalized flows using Equation (7):

$$Z_{i,j,k} = \frac{q_{i,j,k} \cdot \overline{q_{i,j}}}{\sigma_{i,j}}, \quad (7)$$

where Z is the normalized flow, i the number of months (ranging from 1 to 12), k the number of years (ranging from 1931 to 2005), j the number of reservoirs (a total of 8), $q_{i,j,k}$ naturalized flow from station j in month i in year k, $\overline{q_{i,j}}$ is the matrix that represents the average of all the months and ranks, and $\sigma_{i,j}$ is the matrix that represents the standard deviation of the monthly series of all ranks.

The second step was to perform the linear regression of ONS naturalized flows to obtain the parameters of each reservoir that does not have the SMAP calibrated, considering

all other reservoirs as explanatory variables (Itaparica, Sobradinho, Três Marias and Retiro Baixo). The linear regression was given by Equation (8):

$$Z_{i,pj,k} = \sum_{pk=1}^{pk=4} Z_{i,pk,k} \cdot \beta_{i,pk}, \quad (8)$$

where pk are the flows of the four basins obtained through the SMAP model (varying from 1 to 4), pj are the reservoirs that do not have the SMAP calibrated (varying from 1 to 4) and $\beta_{i,pk}$ the regression coefficients.

Figure 5 shows the linear regression model performance in estimating the flows of the four reservoirs that do not have the SMAP model calibrated. It is possible to observe that the Queimado and Xingó reservoirs presented acceptable results. In contrast, in the Moxotó and Complexo Paulo Afonso reservoirs 1, 2, 3 and 4, results were a little below the acceptable value of 0.36, showing 0.34 and 0.35, respectively. Thus, with the coefficients obtained from the ONS naturalized flow series and the flows obtained through the SMAP model with the data from the CMIP6 models, the affluent natural flows for the climate change scenarios for the other reservoirs were obtained using the linear regression parameters.

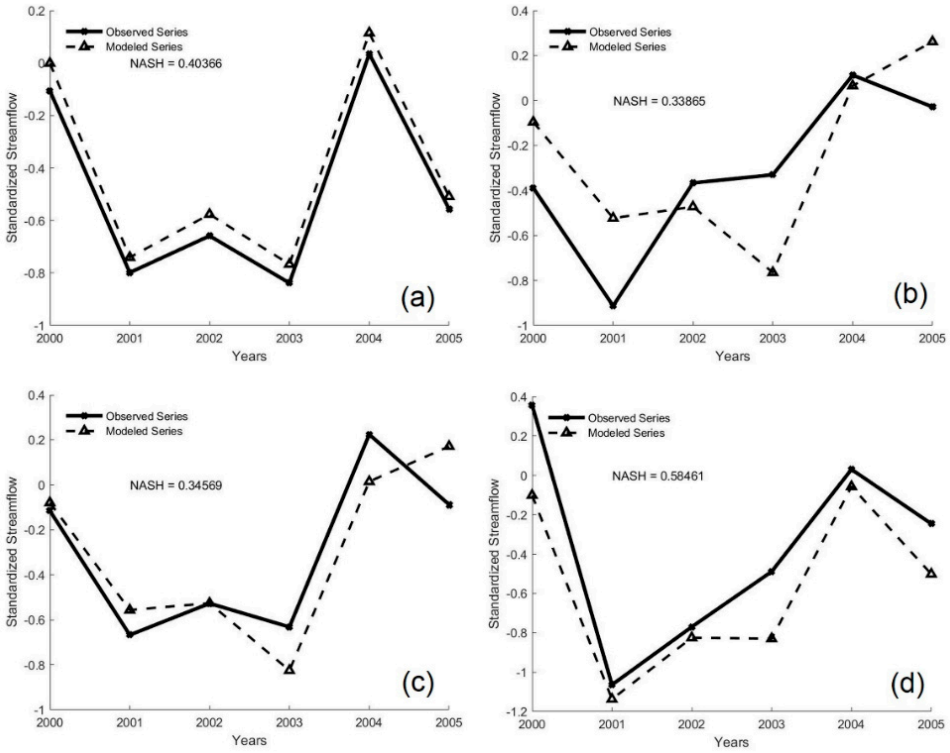

Figure 5. Performance of the linear regression model in the estimation of the annual affluent natural flow of the reservoirs: (**a**) Queimado, (**b**) Moxotó, (**c**) Paulo Afonso Complex, and (**d**) Xingó for the period from 2000 to 2005.

2.8. Consumptive Demands

The withdrawal flows of consumptive demands (irrigation, human supply and industry) from 1961 to 2017 were obtained from ANA for the state municipalities in Brazil and were aggregated in the basin of the reservoirs, see Figure 2. For this purpose, they were quantified through geoprocessing techniques, being expressed through Equation (9):

$$QD_b = \sum_{m=1}^{M} \frac{AB_{mb}}{AT_m} \cdot QD_m, \quad (9)$$

where QD_b is the average flow of demand located inside the basin b (m^3/s); QD_m is the average flow of demand inside the municipality m (m^3/s); AB_{mb} is the area of the municipality m inside the basin b (km^2); and AT_m is the total area of the municipality m (km^2).

The ANA methodology to estimate the consumptive demands was based on investigations of the technical coefficients available in the literature and their compatibility with the data already available [47]. More details on the estimates of the demands are available in the Manual of Consumptive Uses of Water in Brazil in [47], as well as the metadata used in this study.

Four scenarios were considered to analyze the influence of consumptive demands in the future (2018 to 2050) for the river basins that make up the SFRB: Scenario 1 with static demands, i.e., considering the last observed withdrawal flow; Scenario 2 with consumptive demands projected with the exponential smoothing (ETS) model; Scenario 3 with consumptive demands projected with the ETS model considering values below 95% of the confidence interval; and Scenario 4 with consumptive demands projected with the ETS model considering values above 95% of the confidence interval.

The ETS model was proposed in the late 1950s [48–50], and the predictions generated by this model are produced through weighted averages of past observations, with the weights decreasing exponentially as the age of the observations, i.e., the more recent the observation, the greater the associated weight. Thus, being y_T an observation in time T of a time series, the forecast in time T + 1 will be given by:

$$y_{T+1} = \alpha y_T + \alpha(1 - \alpha)y_{T-1} + \alpha(1 - \alpha)^2 y_{T-2} + \ldots, \quad (10)$$

where α is the parameter for smoothing the growth rate that decreases with time.

However, the process has to start at T = 1 with some adjusted value. This adjusted value is called level and is represented by l_0 in Equation (11):

$$Y_{T+1} = \sum_{j=0}^{T-1} \alpha(1 - \alpha)^j y_{T-j} + (1 - \alpha)^T l_0. \quad (11)$$

Moreover, the ETS models are defined in terms of components, making it easier to add extensions, such as trend and seasonality [51]. The name ETS is due to its three parameter extensions: the Error, the Trend and the Seasonal components (E, T, S). These components, in turn, can be: in the Error, Additive (A) or Multiplicative (M) component; in the Seasonal, A or M or none (N) components; and in the Trend, A or M or N component or Dampened Additive (Ad) or Dampened Multiplicative (Md) [51].

Since its creation, with the variation of these components, a total of 30 models have been developed [51–54]. Each model consists of an equation that will describe the data for l_0, trend (b) and seasonality (s) as a function of time t (l_t, b_t, s_t, $s_{t-1}, \ldots, s_{t-m+1}$) using likelihood and space methods for the calculations. In general, these equations are expressed as Equations (12) and (13):

$$y_t = w(x_{t-1}) + r(x_{t-1})\varepsilon_t, \quad (12)$$

$$x_t = f(x_{t-1}) + g(x_{t-1})\varepsilon_t, \quad (13)$$

where y_t is the forecast as a function of a state vector x_t, which will have a transition that describes the states evolution and ε_t is the error associated with white noise.

For an ETS model (A, M, M), that is, with additive error, with tendency and multiplicative seasonal component, the expressions for y_t, l_0, b_t and s_t (Equations (14)–(17)), are:

$$y_t = l_{t-1} b_{t-1} s_{t-m}, \quad (14)$$

$$l_t = l_{t-1} b_{t-1} + \alpha\varepsilon_t / s_{t-m}, \quad (15)$$

$$b_t = b_{t-1} + \beta\varepsilon_t / (s_{t-m} l_{t-1}), \quad (16)$$

$$s_t = s_{t-1} + \gamma\varepsilon_t/(l_{t-1}b_{t-1}), \quad (17)$$

where β and γ are, respectively, the growth parameter of b_t and the component parameter of s_t. For further details on the ETS models equations, please refer to [53].

For this study, ETS was based on the methods described by [53], available through the "forecast" package in the R environment. The best ETS model was chosen with Akaike's information criterion (AIC) (Equation (18)), Schwarz's Bayesian information criterion (BIC) (Equation (19)) and AIC with removed bias (AICc) (Equation (20)).

$$AIC = -2\left(\frac{LL}{T}\right) + \frac{2T_p}{T}, \quad (18)$$

where LL is the log likelihood, T_p is the total of parameters and T is the number of observations.

$$BIC = -2LL + k\ln(T), \quad (19)$$

where k is the estimation of the parameters of the models obtained through the least squares method.

$$AIC_c = AIC + \frac{2(k+2)(k+3)}{T-k-3}, \quad (20)$$

where the expression $\frac{2(k+2)(k+3)}{T-k-3}$ is the bias correction.

2.9. The Decision Support System (SIGA)

The reservoir operation was done through a flow network decision support system named SIGA [23]. It enables the input of different demands and priorities. Furthermore, it provides the supplied durations inherent to the permanence curve of the monthly affluent flows of the reservoirs. The four multiple-use reservoirs of the São Francisco River basin were modeled as a cascade series, as shown in Figure 6. The new demands of the two channels were considered to be met by the system by unifying its uses: human, industrial and irrigation. These uses were also modeled on the downstream stretch of each basin reservoir, through demands.

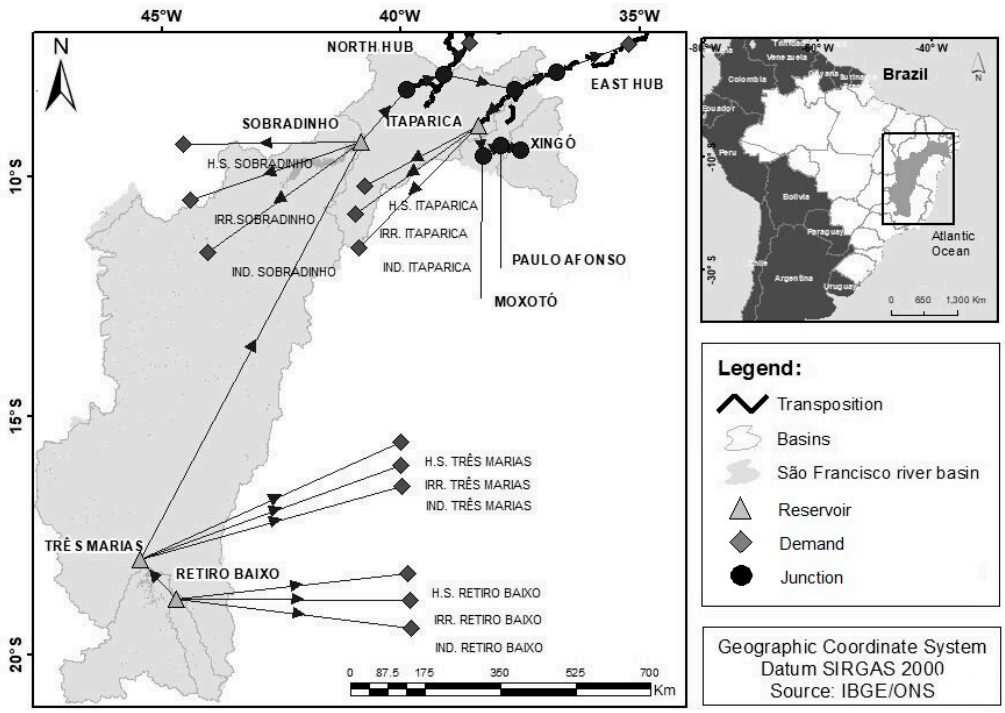

Figure 6. São Francisco River hydrosystem flow network model.

Besides meeting the demands, the modeled system must also need to meet the maximum and minimum discharge limits in the river sections as regulated by the system operator [6], according to Table 3. The values of the minimum limits were used in this study.

Table 3. Operational restrictions downstream studied reservoirs.

Reservoir (m^3/s)	Minimum Discharge (m^3/s)	Maximum Discharge (m^3/s)
Três Marias	100	2500
Sobradinho	700	8000
Itaparica	700	8000

The simulation of the flow network is performed by means of the equation of the water mass balance in reservoirs expressed in Equation (21):

$$V_{t+1} = V_t + I_t - E_t \cdot A_t - R_t - S_t, \quad (21)$$

where V_t is the volume stored at the beginning of time period t (hm^3); V_{t+1} is the volume of the reservoir at the beginning of the next time period t + 1 (hm^3); I_t is the volume affluent to the reservoir during time period t (natural and transfer) (hm^3); E_{t^*} is the evaporated slide during the time period t, assumed constant along the period (hm); A_t is the water surface area at the beginning of period t, assumed constant for short time intervals and function of V_t (hm^2); R_t are the operational withdrawals (hm^3); and S_t is the overflow (withdrawal of uncontrolled water) (hm^3).

The flow network simulations had the operational withdrawals optimized to guarantee the fulfillment of the operational limits, maximize the fulfillment of demands and minimize the evaporated volume, during the chosen simulation periods, through the SIGA software [23]. In order to do so, SIGA uses the multiple objective particle swarm optimization (MOPSO) as an optimization algorithm [23].

During a period of failure to meet the demands, SIGA adopts a system of priorities, from the lowest to the highest, to determine the system nodes that will suffer shortages. This study considered the priority system defined in Table 4, which aims to prioritize human supply over irrigation and industry. The second highest priority was attributed to the new water transfer project, supposedly used to assist other human supply systems of basins.

Table 4. Operational restrictions downstream studied reservoirs.

Consumptive Demand	Priority
Human Supply (HS)	1
Transposition (TR)	2
Irrigation (IRR)	3
Industry (IND)	4

2.10. Hydroelectric Energy Production

Conventionally, the power produced in a HPP is given by:

$$ph = G \cdot \eta_t \cdot hl \cdot q, \quad (22)$$

where G is a constant with a value of $9.81.10^{-3}$ (kg/m^2s^2) that represents the product between the density of the water (1000 Kg/m^3), the gravity (g) and constant with a value of 10^6 that converts the energy of (J) into (MJ); η_t is the hydraulic performance of the turbine; hl is the penstock head loss (m); q is the turbine flow in only one generating unit (m^3/s).

Usually, the net drop height has been represented using fourth-order polynomials depending on the stored volume (in the upstream level) and the discharged flow (in the downstream level). The following polynomial gives the value of the upstream level:

$$fcm = a_0 + a_1 \cdot V + a_2 \cdot V^2 + a_3 \cdot V^3 + a_4 \cdot V^4, \quad (23)$$

where fcm is the value of the upstream level (m); $a_0, \ldots, a_4$ are the coefficients of the polynomial that represents the upstream level for the reservoir; V is the stored volume (hm^3).

On the other hand, the downstream level of the plant is the river level after the turbine. The same can be given through the polynomial that relates the discharged flow (turbine flow—Q plus spilling flow—S into the HPP) with the respective coefficients:

$$fcj = b_0 + b_1(Q + S) + b_2(Q + S)^2 + b_3(Q + S)^3 + b_4(Q + S)^4, \quad (24)$$

where fcj is the value of the downstream elevation (m); S is the spilled flow rate from the HPP (m^3/s); b0 ... b4 are the coefficients of the polynomial that represents the downstream elevation to the reservoir.

Thus, based on Equations (23) and (24), the forebay elevation (m) becomes:

$$hb = fcm - fcj \quad (25)$$

However, not all of this forebay elevation is available at the turbine entrance, as part of it is lost when the water passes through the forced conduit and other through penstock head loss. The net fall height of the HPP is defined as the difference between hb and the hydraulic loss, expressed by:

$$hl = hb - pl, \quad (26)$$

where pl is the hydraulic net loss (m).

The hydraulic losses, in turn, were modeled as a quadratic function of the turbine flow and a certain constant, as follows:

$$pl = k_p \cdot q^2 \quad (27)$$

where k_p is a constant that depends on the physical characteristics of the forced duct that connects the reservoir to a certain HPP (s^2/m^5).

As for the turbine performance, to build a model closer to the reality of the hydraulic performance, two variables must be taken into consideration: the net drop height it is submitted to and its turbine flow [55]. Thus, this data set is represented through the following concave quadratic function:

$$\eta_t = r_0 + r_1 \cdot q + r_2 \cdot hl + r_3 \cdot q \cdot hl + r_4 \cdot q^2 + r_5 \cdot hl^2 \quad (28)$$

where $r_0, \ldots, r_5$ are the coefficients of the polynomial that represent the yield of a given hydroelectric unit.

The values of the coefficients of the polynomials that are upstream (variable "a", Equation (23)), downstream (variable "b", Equation (24)) and the efficiency of the turbine (variable "r", Equation (28)) for each reservoir, as well as the constants used to obtain the hydraulic loss (variable "kp", Equation (27)), are in Table 5.

These levels were represented through fourth-degree polynomials, obtained through polynomial regression. The turbine-generator yield (%) of HPP Itaparica, provided by [55], equivalent to η equal to 91%, was used. The kp constant to obtain the hydraulic losses, belonging to Equation (28), considered the kp values of 2.53×10^{-5}, for HPP Três Marias; 9.84×10^{-7}, for HPP Sobradinho; and 0 for HPP Itaparica, which made pl equal to zero, that is, without losses.

Table 5. Values of polynomial coefficients.

Reservoir	Três Marias			Sobradinho			Itaparica	
Coefficient	**a**	**b**	**r**	**a**	**b**	**r**	**a**	**b**
0	5.3×10^{2}	5.2×10^{2}	3.6×10^{-1}	3.7×10^{2}	3.6×10^{2}	3.6×10^{-1}	2.8×10^{2}	2.5×10^{2}
1	6.1×10^{-3}	1.6×10^{-3}	7.0×10^{-3}	1.4×10^{-3}	2.0×10^{-3}	1.4×10^{-3}	6.8×10^{-3}	-
2	-4.8×10^{-7}	-2.6×10^{-7}	7.0×10^{-3}	-5.4×10^{-8}	-3.0×10^{-7}	1.3×10^{-2}	-8.9×10^{-7}	-
3	2.2×10^{-11}	2.9×10^{-11}	4.7×10^{-5}	1.2×10^{-12}	2.5×10^{-11}	1.8×10^{-5}	7.0×10^{-11}	-
4	-3.9×10^{-16}	-1.2×10^{-15}	-4.3×10^{-5}	-9.6×10^{-18}	-7.7×10^{-16}	-1.8×10^{-6}	-2.2×10^{-15}	-
5	-	-	-1.2×10^{-4}	-	-	-4.0×10^{-4}	-	-

Source: [55].

Figure 7 shows the validation with the NASH coefficient obtained comparing the estimation of the energy generated by Itaparica, Sobradinho and Três Marias HPP obtained through the SIGA software with the observed series obtained from ONS in the period 1999 to 2016.

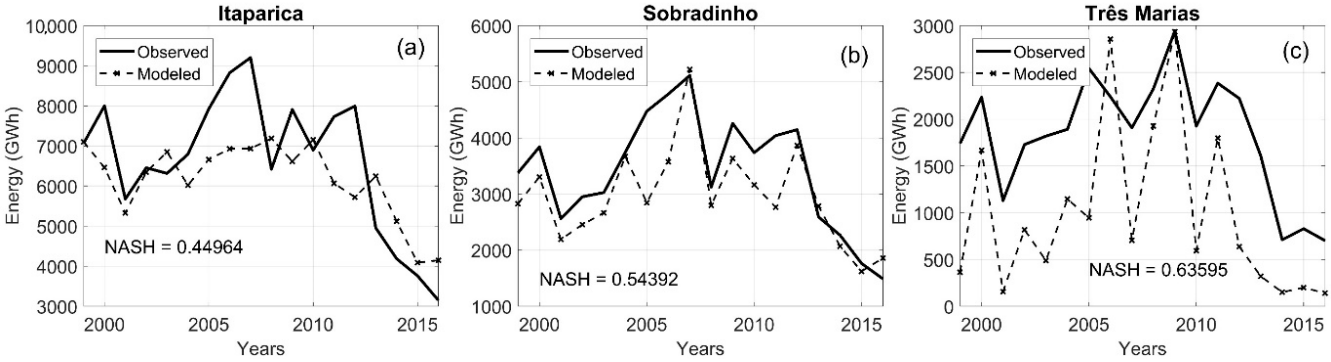

Figure 7. Comparison of the estimates of the annual energy production by the (**a**) Itaparica, (**b**) Sobradinho and (**c**) Três Marias hydroelectric power plants for the period 1999 to 2016 with the SIGA software.

As NASH prioritizes the maximum values of the time series [56], even the hydroelectric power generated with the model presenting discrepancies in Três Marias when compared to the observed hydroelectric power, the maximum values were well represented, resulting in NASH of approximately 0.64.

2.11. Projection Analysis

The analysis of the projections of the affluent natural flows and hydroelectric energy were carried out for the four reservoirs and the three main HPP of the São Francisco River, through the Mann–Kendall Sen test, Q90 and percentage anomaly.

2.11.1. The Mann–Kendall Sen Test

The non-parametric Mann–Kendall Sen test was used to check trends in the flow series. According to [57], the nonparametric Mann-Kendall-Sen test has been widely used for hydrological studies and is recommended by the WMO.

Therefore, according to [58], the statistics of the Mann-Kendall test for a series (Z1, Z2, . . . , Zn) coming from a sample of n independent random variables and identically distributed, is given by Equation (29):

$$S = \sum_{i=1}^{n-1} \sum_{j=i+1}^{n} \text{sinal}(Z_j - Z_i), \quad (29)$$

where S are the values of the series in annual time intervals; i and j are the time indexes, and n is the number of series elements [57]. The term sign $(Z_j - Z_i)$ is the result of Equation (30):

$$\text{signal}(Z_j - Z_i) = \begin{cases} +1 \text{ se } (Z_j - Z_i) > 0 \\ 0 \quad \text{se } (Z_j - Z_i) = 0 \\ -1 \text{ se } (Z_j - Z_i) < 0 \end{cases} \quad (30)$$

For the null hypothesis test H0 (which considers not having a positive trend), the TAU variables and p-value were used. The TAU variable is related to the correlation classification coefficient and quantifies the monotonic association, being given by Equation (31):

$$\text{TAU} = \frac{S}{\frac{1}{2}n(n-1) - \sum_{i=1}^{g} t_i}, \quad (31)$$

where n is the size of the series.

H0 is accepted in the Mann–Kendall TAU when the test is less than a critical value named α, which for this study was $\alpha = 0.05$ (for a statistical significance of 95%), that is, for TAU < α, the series has no positive trend. Otherwise, i.e., for TAU $\geq \alpha$, the time series has a positive tendency. Otherwise, the p-value of the statistic S considers the H0 true, for p-value > α and false for *p*-value $\leq \alpha$ [57].

The Sen estimator provides the magnitude of the detected trends. According to [57], it is estimated through the statistic Q, given by Equation (32):

$$Q_{ij} = \frac{X_j - X_i}{j - i}, \text{ with } i < j, \quad (32)$$

where X_i and X_j are related to the values of the variable under study in times i and j [57]. The positive or negative value for Q indicates increasing or decreasing tendency, respectively.

2.11.2. Permanence Curve and Regularized Flow (Q90)

The performance of the system was measured in terms of meeting the consumptive demands during the observed period and in two future scenarios: (i) the possible increase of gas emissions that intensify the study effect (SSP2-4.5 and SSP5-8.5); and (ii) possible future annual consumptive demands (D1, D2, D3 and D4). The indicator used to measure this degree of service was the permanence curve (PC).

The permanence curve or duration of flows is equivalent to a hydrogram of the accumulated frequency of flows in a river [59]. The same is expressed through the relationship between the flow and the frequency (empirical estimate) with which this flow is exceeded or equalized, such as:

$$\text{PC} = \frac{m}{n} \times 100, \quad (33)$$

where m is the order of the ordered value and n is the number of the series values. This study used monthly flows.

PC helps in the flow data analysis when the percentage of time the river has flows in a given range is required or what percentage of time a river has sufficient flow to meet a given demand [59]. In this study, PC was used to obtain the flow that is exceeded 90% of the time, which is called regularized flow or Q90. This has been used as a reference for legislation in environment and water resources in most Brazilian states and provides a flow duration that supplies 90% of the time to end-users.

2.11.3. Anomaly Percentage

For the statistical analysis of the annual energy projections, the calculation of anomaly percentage was used. It is expressed in Equation (27) and used the CMIP6 model projections related to scenarios SSP2-4.5 and SSP5-8.5 and the demands D1, D1, D3 and D4 in the period

from 2021 to 2050 (21st century). A comparison is made with the representation of the 20th century (1901 to 2000) simulated by CMIP6 models using historical simulated data.

$$A_{annual} = \frac{(E^a_{XXI} - E^a_{XX})}{E^a_{XX}} \times 100, \quad (34)$$

where E^a_{XXI} is the annual average energy of the projections for the scenarios of the 21st century and E^a_{XX} is the annual average energy of the of the 20th century.

3. Results

3.1. Streamflow

The observed historical time series of affluent natural flows for the period 1931 to 2019 (see Figure 8) show high inter-annual variability, with maximum values close to 5000 m^3/s in the reservoirs of Itaparica and Sobradinho, above 1500 m^3/s in Três Marias and close to 350 m^3/s in Retiro Baixo. The minimum values were below 1000 m^3/s in the reservoirs of Itaparica and Sobradinho, 500 m^3/s in Três Marias and 100 m^3/s in Retiro Baixo, and they were all registered in the last years. This fact reflects the prolonged water scarcity that has reached the SFRB in recent years, especially in those basins that are totally or partially inserted in the semi-arid region, such as the Itaparica and Sobradinho. In those basins, the Mann–Kendall Sen test indicated a negative trend.

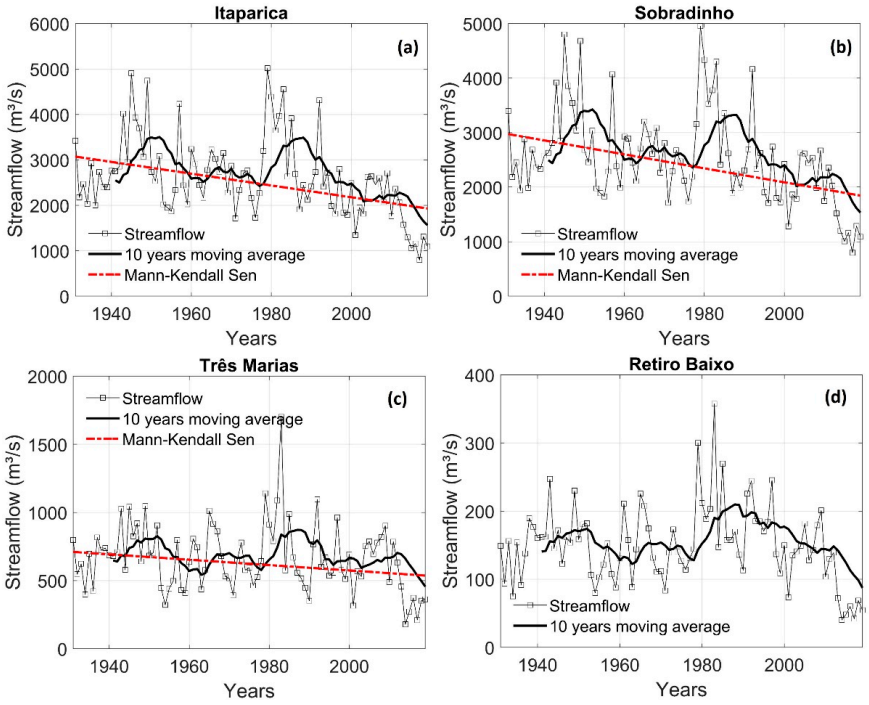

Figure 8. Historical annual estimation of Brazilian National Electrical System Operator (ONS) series of naturalized flow with 10-year moving average and Mann–Kendall Sen trend test (from 1931 to 2019); (**a**) Itaparica, (**b**) Sobradinho, (**c**) Três Marias and (**d**) Retiro Baixo.

In addition, a decadal variability with well-defined periods was observed, with higher values of affluent natural flows between 1930 and 1960 and between 1980 and 1995 and lower flows between 1960 and 1990 in all reservoirs, which coincided with the phases of the Atlantic Multidecadal Oscillation (AMO) and the Pacific Decadal Oscillation (PDO) [15,32,60,61]. According to [60], the period from 1930 to 1960 adjusted to the positive phase of AMO (with higher temperatures in the tropical Atlantic Ocean) with the drought period in the NBR, while the lower temperatures of the tropical Atlantic Ocean, i.e., the negative phase of AMO, coincided with greater rainfall in the region from 1960 to 1990. According to [15,61], the last positive phase of AMO occurred from 1995 onwards and still

continues. Therefore, the low values of affluent natural flows observed may be partly due to AMO's positive phase and the expected higher Sea Surface Temperatures (SST) in the tropical Atlantic Ocean.

However, even with the decadal cycle indicating a phase with lower affluent natural flows since 1995, this positive phase of AMO is unprecedented and may be attributed to the extreme increase in global SST associated with anthropogenic global warming [15,61].

Figure 9 shows the trend declivities of the CMIP6 models for the SSP2-4.5 and SSP5-8.5 scenarios (from 2017 to 2100) concerning the history (period from 1901 to 2000) of the affluent natural flows of the studied reservoirs, according to the Mann–Kendall Sen test. For the set of models that showed a significant trend, the increase in greenhouse gas emissions suggests a more significant impact on flows. In most cases, the slope module is larger for the SSP5-8.5 scenario than for the SSP2-4.5 scenario. This fact may be related to the considerable temperature increase projected by the SSP5-8.5 scenario, resulting in increased PET projected for the 21st century. This result was also found with the CMIP5 data by [17]. The MIROC6 and MRI-ESM2-0 models indicated a positive trend. In contrast, the other models projected a negative trend, with the declivity of the CanESM5 model presenting a value below −30 for the Queimado, Sobradinho, Itaparica, Moxotó, Xingó and Complexo Paulo Afonso reservoirs.

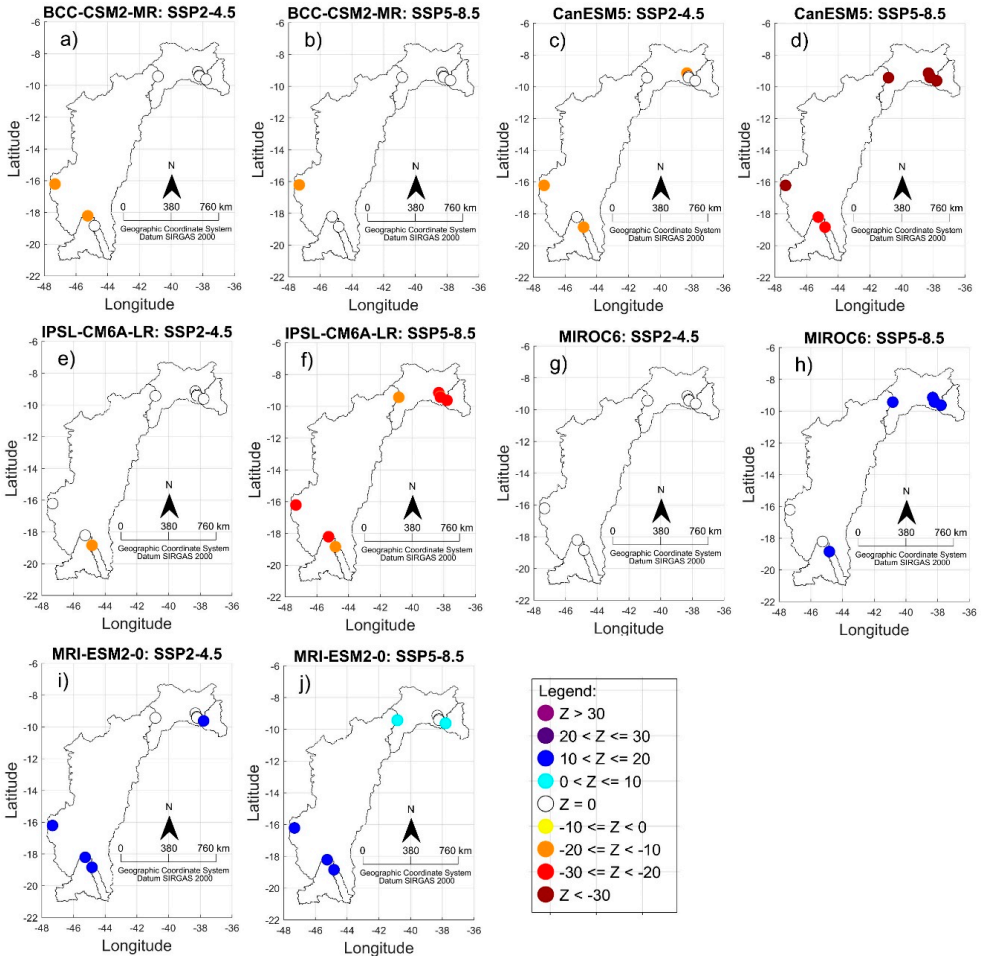

Figure 9. Trend, according to the Mann–Kendall Sen method of the standardized annual streamflow average, referring to the SSP2-4.5 and SSP5-8.5 scenarios of the CMIP6 (Intercomparison Model Project) for the period 2017–2100; (**a**) BCC-CSM2-MR: SSP2-4.5, (**b**) BCC-CSM2-MR: SSP5-8.5, (**c**) CanESM5: SSP2-4.5, (**d**) CanESM5: SSP5-8.5, (**e**) IPSL-CM6A-LR: SSP2-4.5, (**f**) IPSL-CM6A-LR: SSP5-8.5, (**g**) MIROC6: SSP2-4.5, (**h**) MIROC6: SSP5-8.5, (**i**) MRI-ESM2-0: SSP2-4.5, (**j**) MRI-ESM2-0: SSP5-8.5.

Figure 10 presents the box-plots of the ratio between Q90 for the SSP2-4.5 and SSP5-8.5 scenarios varying in 30 years (2021–2050 and 2051–2080), respectively, and Q90 in the historical period (1901–2000) for the SFRB reservoirs, corresponding to the five models analyzed. The models indicated reductions in Q90 for most of the SFRB reservoirs and the two analyzed periods. The exception was the Itaparica reservoir, which for the SSP5-8.5 scenario from 2021 to 2050, the model median indicated an increase in Q90. The increase in Q90 presented by the Itaparica basin may be related to the low calibration of the SMAP model (with a low NASH index of 0.36 according to Table 2), since this basin is located below Sobradinho and the water transfer project for the semi-arid region of the NRB, for which the expectation would be a decrease in Q90.

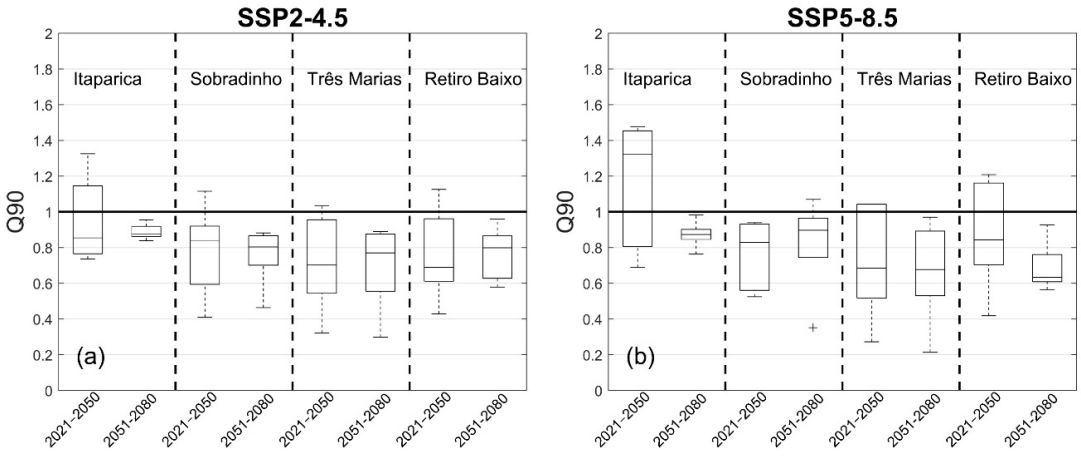

Figure 10. Ratio between the flow rate: (**a**) with 90% duration of the future scenario models SSP2-4.5 (2021–2050 and 2051–2080) and the flow rate with 90% duration of the control period of the Historical models (1901–2000) and (**b**) with 90% duration of the future scenario models SSP5-8.5 (2021–2050 and 2051–2080) and the flow rate with 90% duration of the control period of the Historical models (1901–2000). The continuous horizontal line represents the situation without future change, with a ratio equal to 1.

3.2. Projection of Consumptive Demands

In the historical time series, annual consumptive demands withdrawn from 1961 to 2017 increased over time, as shown in Figures 11–14 and Table 6. The demand for irrigation had the highest average annual growth rates: 6.80%, 7.42%, 10.99% and 9.29% in Itaparica, Sobradinho, Três Marias and Retiro Baixo, respectively. It is also the irrigation demand that has the highest values in three of the four analyzed reservoirs. The exception was the Retiro Baixo reservoir, where the human demand exceeded the others.

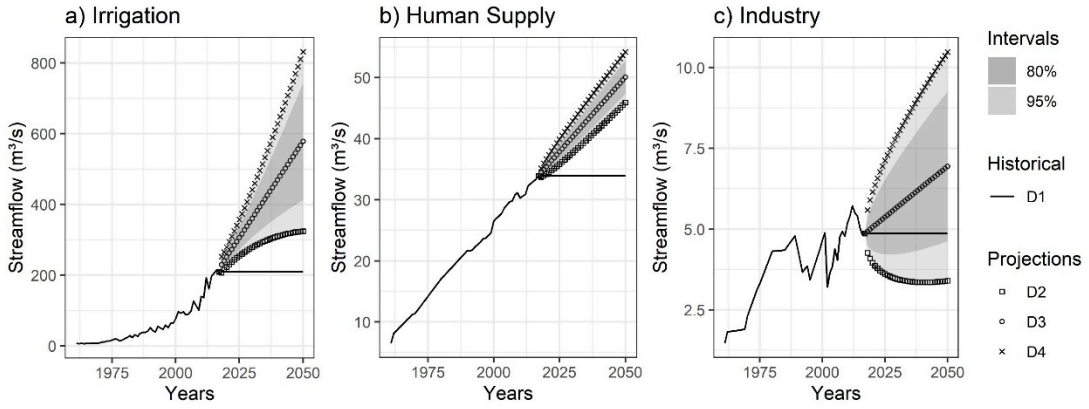

Figure 11. Scenarios of the projections of annual consumptive demands on the Sobradinho reservoir using the exponential smoothing (ETS) model for the period 2018 to 2050.

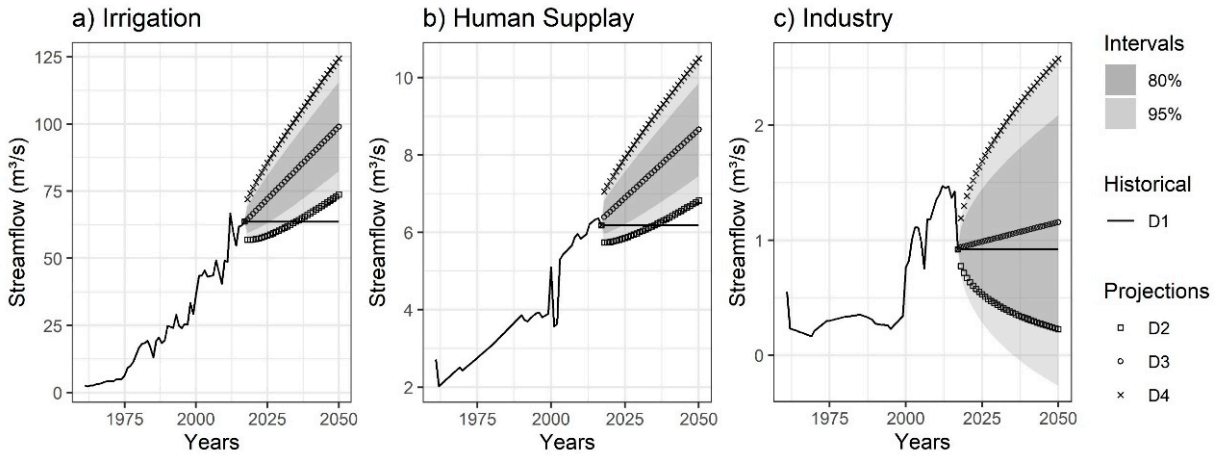

Figure 12. Scenarios of the projections of annual consumptive demands on the Itaparica reservoir using the ETS model for the period 2018 to 2050.

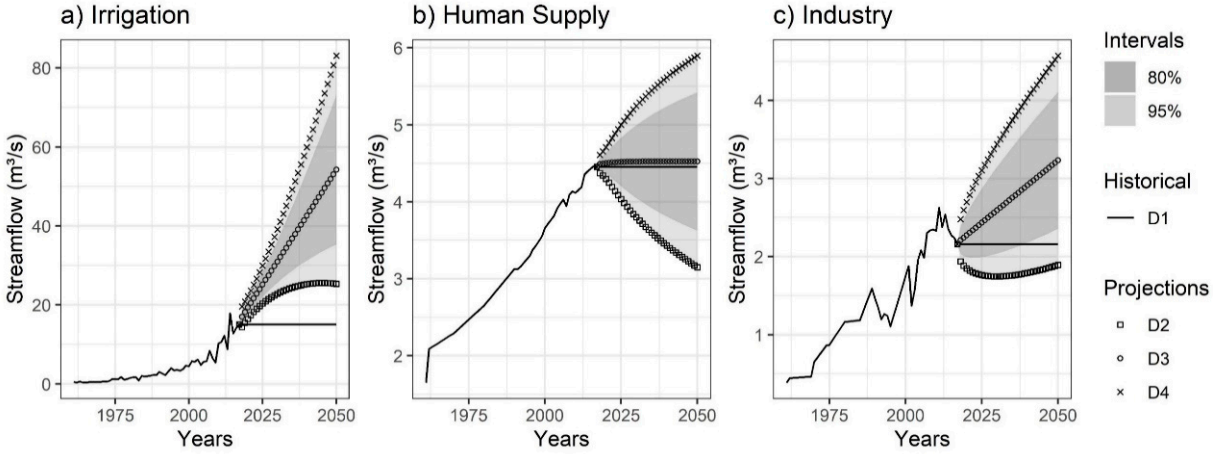

Figure 13. Scenarios of the projections of annual consumptive demands on the Três Marias reservoir using the ETS model for the period 2018 to 2050.

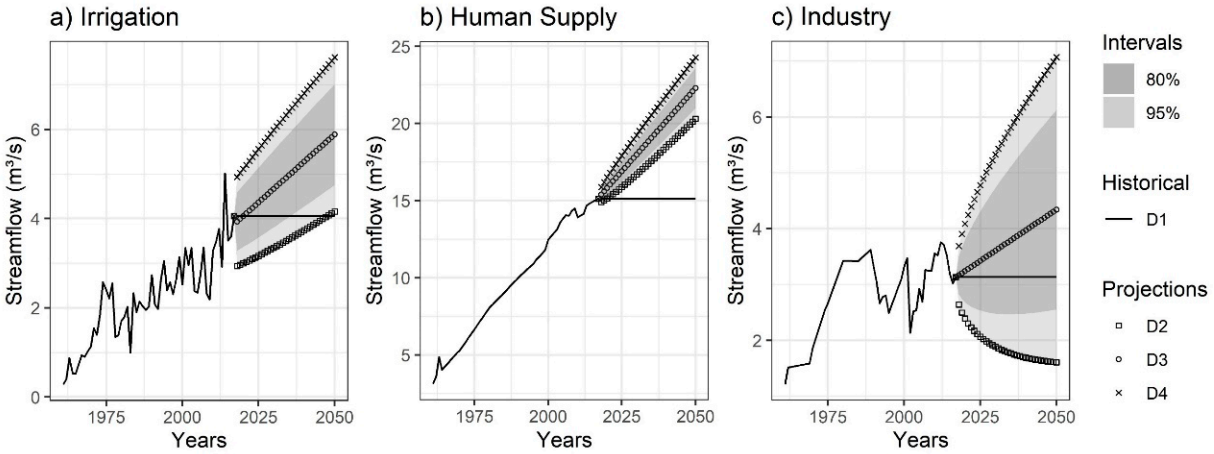

Figure 14. Scenarios of the projections of annual consumptive demands on the Retiro Baixo reservoir using the ETS model for the period 2018 to 2050.

Table 6. Average annual growth rate of consumptive demands.

Reservoir	Demands	Average Annual Growth Rate (%)			
		Historical (1961–2017)	D2	D3	D4
Itaparica	Irrigation	6.80	0.81	1.35	1.73
	Human Supply	1.88	0.54	0.95	1.25
	Industry	2.87	−3.73	0.66	2.46
Sobradinho	Irrigation	7.42	1.41	2.93	3.80
	Human Supply	3.03	0.97	1.18	1.36
	Industry	2.53	−0.70	1.07	1.99
Três Marias	Irrigation	10.99	1.80	3.70	4.62
	Human Supply	1.84	−1.02	0.02	0.77
	Industry	3.53	−0.08	1.19	1.93
Retiro Baixo	Irrigation	9.29	1.10	1.27	1.37
	Human Supply	2.99	0.97	1.16	1.34
	Industry	2.15	−1.53	0.99	2.06

The ETS model projected growth scenarios for the period 2018 to 2050 for most of the consumptive demands. The exception was the D2 scenario (more optimistic). In this scenario, industrial demands reduced its withdrawals with an average annual rate of −3.73%, −0.70%, −0.08% and −1.53% for the reservoirs of Itaparica, Sobradinho, Três Marias and Retiro Baixo, respectively. Human supply also showed a reduction on the average annual rate of −1.02% for the reservoir of Três Marias in the D2 scenario.

3.3. Hydroelectric Energy Production

Future hydroelectric energy production considered CMIP6 climatic scenarios SSP2-4.5 and SSP5-8.5 (in the period from 2021 to 2050), and projected demands of D1, D2, D3 and D4 scenarios relative to the historical period from 1901 to 2000. Figure 15 indicates the anomalies behavior in the average percent of the hydroelectric energy produced at Itaparica, Sobradinho and Três Marias HPP.

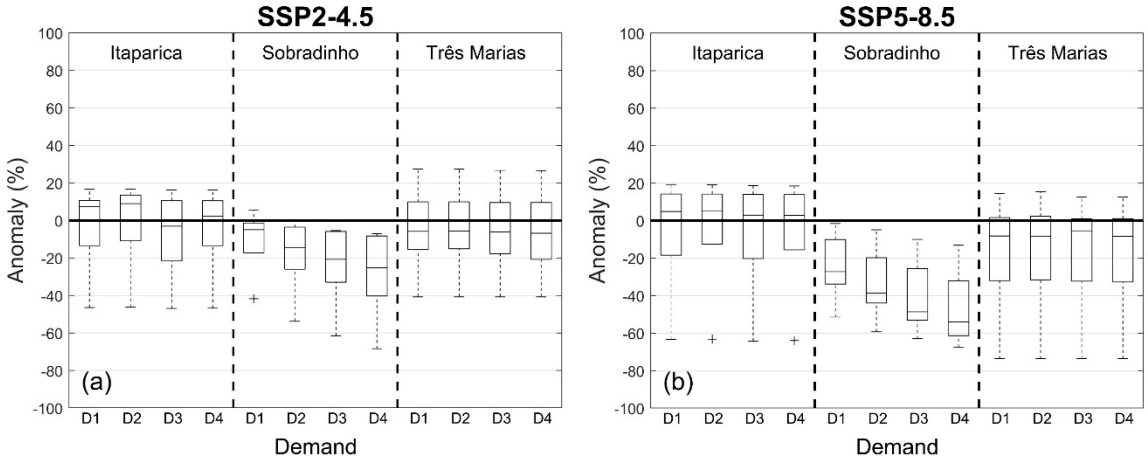

Figure 15. Annual percentage anomaly of the Energies of Itaparica, Sobradinho and Três Marias HPP obtained with the SIGA software with the projections of the consumptive demands D1, D2, D3 and D4 with the scenario: (**a**) SSP2-4.5 and (**b**) SSP5-8.5 in the period from 2021 to 2050 referring to the historical period from 1901 to 2000.

The SSP5-8.5 scenario models indicated more intense reductions of hydropower than the SSP2-4.5 scenario for two, out of the three HPP analyzed in this study. Itaparica HPP was the only exception, with the models indicating, for the two scenarios of future climate and most scenarios of consumptive demands, an increase of hydropower generation.

For the consumptive demands, Sobradinho's HPP was the one that showed the highest sensitivity to future scenarios of these demands. It presented a more significant decrease in the hydroelectricity generation when the demands became more pessimistic. The D4 scenario presented greater intensity of the decrease in hydroelectric power with a median of less than −50%. For Três Marias and Itaparica HPP, there was little change of the consumptive demands, with the medians of the anomalies close to −10% and 10%, respectively, in the two climate scenarios (SSP2-4.5 and SSP5-8.5).

Figure 16 shows the trend slopes of the CMIP6 models for the future climate scenarios SSP2-4.5 and SSP5-8.5 and the consumptive demands D1, D2, D3 and D4 using the Mann–Kendall Sen test of the energies of the Itaparica, Sobradinho and Três Marias HPP.

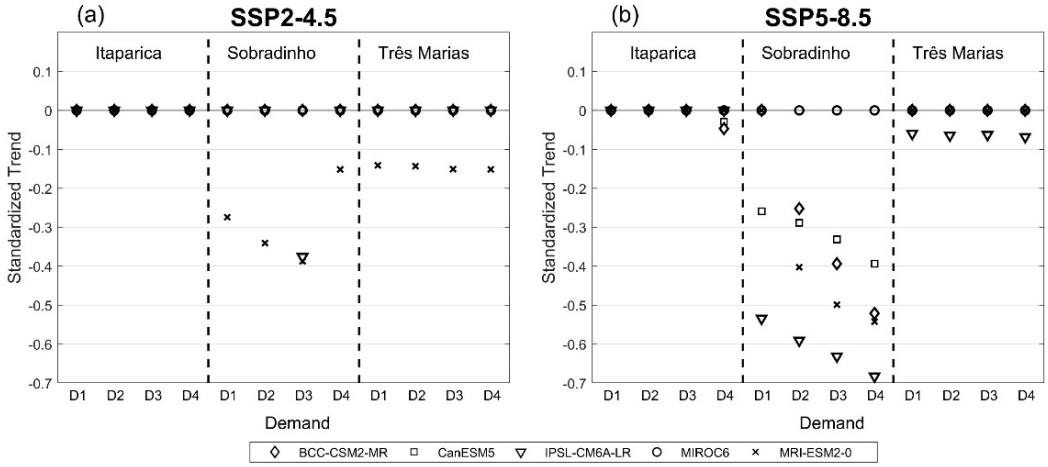

Figure 16. Trend, according to the Mann–Kendall Sen method of the standardized annual energy hydropower, referring to the: (**a**) SSP2-4.5 and (**b**) SSP5-8.5 Scenarios of the CMIP6 for the period 2021–2050. D1, D2, D3 and D4 are projections of consumptive demands.

From the set of models with a significant trend, there is clear evidence that at Sobradinho HPP, the increase in greenhouse gas emissions suggests a more significant impact on electricity generation since the slope module is higher for the SSP5-8.5 scenario than for the SSP2-4.5. Sobradinho HPP also had the greater magnitude of the slope modules for the most pessimistic consumptive demands scenarios.

Among the models that indicated reductions in electricity generation, the IPSL-CM6A-LR model stands out, reaching the −0.7 slope module in scenario D4. In the Três Marias UH, for the SSP2-4.5 scenario, only the MRI-ESM2-0 model presented a significant trend with a negative slope in all scenarios of consumptive demands. In contrast, in the SSP5-8.5 scenario, only the IPSL-CM6A-LR model presented a significant trend, which was also negative. In the Itaparica HPP, only in the SSP5-8.5 climate scenario and in the D4 demand scenario, the BCC-CSM2-MR and CanESM5 models presented a significant trend with negative declivities close to −0.05.

4. Conclusions

The impacts of climate change in the coming decades may influence the intensification of extreme events such as floods, droughts and temperature increases. Climate change, added to an increase in consumptive demands caused by population and wealth growth, can put significant pressure on the hydrosystems, especially when amplified by additional new demands from water transfer projects. Such a situation can significantly influence hydroelectric generation. Thus, this study aimed at generating information on the impact of these changes (climate and demand) upon SFRB's electricity production. Decision-makers can use such information to adopt energy policies and measures to mitigate the possible impacts of such scenarios.

In the time series of affluent natural flows observed in the period from 1931 to 2016, the minimum annual flows of the Itaparica, Sobradinho, Três Marias and Retiro Baixo reservoirs were presented during the last six years. Negative trends, according to the Mann–Kendall Sen test, were found for the first two reservoirs. This period of drought over the NBR has already been reported in several studies, in which they relate to the low-frequency natural variability of the positive phase of the PDO and AMO atmospheric phenomena [15,60,61]. However, according to [15] and [61], this positive phase of AMO and PDO is unprecedented and may be attributed to the extreme increase in global SSM due to anthropogenic global warming.

As a consequence of the prolonged drought, in 2016 ANA reduced the flow of the São Francisco River from 800 m^3/s to 700 m^3/s [6] and in May 2017 to 600 m^3/s [25].

This reduction in affluent natural flows continues in both climate scenarios, SSP2-4.5 and SSP5-8.5, from 2017 to 2100 compared to the historical period (from 1901 to 2000) of the CMIP6 models. The set of models indicated reductions in Q90 for most SFRB reservoirs and in the two periods analyzed (2021–2050 and 2051–2100). Except for the Itaparica reservoir, which for the SSP5-8.5 scenario, from 2021 to 2050, the median of models indicated an increase in Q90. For the set of models that presented a significant trend according to the Mann–Kendall Sen test, an increase in greenhouse gas emissions suggests a more significant impact on the affluent natural flows because the slope module is greater for scenario SSP5-8.5 than for scenario SSP2-4.5.

The analyses of the historical time series of flows taken for the consumptive demands from 1961 to 2016 showed an exponential increase in these demands. Irrigation demands presented the highest average annual growth rates, with values of 6.80%, 7.42%, 10.99% and 9.29% for the reservoirs of Itaparica, Sobradinho, Três Marias and Retiro Baixo, respectively. According to [24], about 77% of the current total demand from the São Francisco River is for irrigation, 11% for urban demand and 7% for industrial demand.

Four possible scenarios of these consumptive demands were projected for 2017 to 2051, coupled with the future climate scenario (SSP2-4.5 and SSP5-8.5). For the SSP5-8.5 scenario, the models indicated projections with more intense hydropower reductions than the SSP2-4.5 scenario at the Sobradinho and Três Marias HPP. The exception was the Itaparica HPP, in which the models indicated, for the two future climate scenarios and for most scenarios of consumptive demands, an increase in hydroelectric power. The Sobradinho HPP was the one that showed the highest sensitivity to the future scenarios of consumptive demands, presenting greater intensity in the decrease of hydroelectric energy. In contrast, the demand scenarios were more pessimistic, i.e., scenario D4 presented greater intensity in the decrease of hydroelectric generation with a median of less than –50%, to the detriment of the other scenarios of consumptive demands D1 (no change in demands from 2016) with approximately −30%, D2 with approximately −40% and D3 with approximately −50% in scenario SSP5-8.5.

The possible reduction in water and energy availability and the increase in consumptive demands, especially irrigation demand, reveals that future conflict may intensify among multiple uses. Moreover, possible economic downturn due to water reduction for agriculture and industry, shortage of municipal water supply and crisis in the region's electricity sector are possible future outcomes.

The need for new policies to restrict irrigation growth in SFRB and to prevent and oppose illegal water abstraction is evident. As far as hydroelectric power generation is concerned, with the increase in the need for water to meet consumptive demands, it is necessary to increasingly invest in alternative forms of electricity generation to supply this reduction in hydroelectric generation.

Two possibilities to increase future energy generation can be implemented, resulting in positive and negative climate change feedback. Positive feedback for climate change would be an investment in non-renewable energy, such as generating thermal energy that uses fossil fuels and emits CO_2 into the atmosphere. In 2015, this energy type accounted for 47% of all energy generated in the NEB region. The other possibility facing these scenarios and

with negative feedback for climate change would be the massive investment in renewable sources such as wind and solar. In 2018 the wind energy share was already approximately 52% in the region [9]. This type of energy in Brazil, according to [62], is already cheaper than electricity generated from fossil fuel, biomass and nuclear sources.

Overall, this study showed that climate change associated with growing consumptive demands both from existing and new users may significantly affect hydroelectricity production in SFRB. In an uncertain future, proactively planning how the water–energy–food nexus will interact in the next decades is key to promote a sustainable future for our society. Our results support a necessity to invest in renewable energy to account for the hydroelectric production losses and invest in irrigation regulations as the main consumptive user in the region.

Author Contributions: Conceptualization, methodology and validation, M.V.M.d.S. and C.d.S.S.; software, M.V.M.d.S. and J.M.F.d.C.; formal analysis, investigation, resources, data curation, M.V.M.d.S., J.M.F.d.C. and C.d.S.S.; writing—original draft preparation, M.V.M.d.S. and C.d.S.S.; writing—review and editing, visualization and supervision, C.d.S.S., E.S.P.R.M. and F.d.C.V.J. All authors have read and agreed to the published version of the manuscript.

Funding: This research was funded by Fundação Cearense de Apoio ao Desenvolvimento Científico e Tecnológico (FUNCAP) (grant number 001), and the Conselho Nacional de Desenvolvimento Científico e Tecnológico -Brasil (Uma análise sobre nexo: Clima, água e energia na bacia do rio São Francisco Project, No. 310286/2018-2).

Institutional Review Board Statement: Not applicable.

Informed Consent Statement: Not applicable.

Data Availability Statement: The study did not report any data.

Acknowledgments: The authors thank the Search Group "Gerenciamento do Risco Climático para a Sustentabilidade Hídrica" of Federal University of Ceará coordinated by Francisco de Assis de Souza Filho.

Conflicts of Interest: The authors declare no conflict of interest.

References

1. IPCC. Summary for policymakers. In *Managing the Risks of Extreme Events and Disasters to Advance Climate Change Adaptation*; Special Report Intergovernmental Panel on Climate Change; Cambridge University Press: Cambridge, UK, 2014; pp. 3–22. [CrossRef]
2. Schaefli, B. Projecting hydropower production under future climates: A guide for decision-makers and modellers to interpret and design climate change impact assessments. *WIREs Water* **2015**, 1–25. [CrossRef]
3. Marengo, J.A.; Cunha, A.P.M.A.; Nobre, C.A.; Ribeiro Neto, G.G.; Magalhaes, A.R.; Torres, R.R.; Sampaio, G.; Alexandre, F.; Alves, L.M.; Cuartas, L.A.; et al. Assessing drought in the drylands of northeast Brazil under regional warming exceeding 4 °C. *Nat. Hazards* **2020**, *103*, 2589–2611. [CrossRef]
4. Pontes Filho, J.D.; de Souza Filho, F.A.; Martins, E.S.P.R.; Studart, T.M.C. Copula-Based Multivariate Frequency Analysis of the 2012–2018 Drought in Northeast Brazil. *Water* **2020**, *12*, 834. [CrossRef]
5. Campos, J.N.B. Paradigms and Public Policies on Drought in Northeast Brazil: A Historical Perspective. *Environ. Manag.* **2015**, *55*, 1052–1063. [CrossRef] [PubMed]
6. ONS. *Plano de Operação Energética 2019–2023*; ONS: London, UK, 2019; Volume 36.
7. BRASIL. Projeto de Integração doRio São Francisco; RIMA: Belo Horizonte, MG. July 2004. Available online: https://antigo.mdr.gov.br/images/stories/ProjetoRioSaoFrancisco/ArquivosPDF/documentostecnicos/RIMAJULHO2004.pdf (accessed on 28 January 2021).
8. Jong, P.; Tanajura, C.A.S.; Sánchez, A.S.; Dargaville, R.; Kiperstok, A.; Torres, E.A. Hydroelectric production from Brazil's São Francisco River could cease due to climate change and inter-annual variability. *Sci. Total Environ.* **2018**, *634*, 1540–1553. [CrossRef]
9. ONS. *Geração de Energia*; ONS: London, UK, 2020.
10. Kuriqi, A.; Pinheiro, A.N.; Sordo-Ward, A.; Garrote, L. Water-energy-ecosystem nexus: Balancing competing interests at a run-of-river hydropower plant coupling a hydrologic–ecohydraulic approach. *Energy Convers. Manag.* **2020**, *223*. [CrossRef]
11. Yuan, M.H.; Lo, S.L. Ecosystem services and sustainable development: Perspectives f1 rom the food-energy-water Nexus. *Ecosyst. Serv.* **2020**, *46*, 101217. [CrossRef]
12. Karabulut, A.A.; Crenna, E.; Sala, S.; Udias, A. A proposal for integration of the ecosystem-water-food-land-energy (EWFLE) nexus concept into life cycle assessment: A synthesis matrix system for food security. *J. Clean. Prod.* **2018**, *172*, 3874–3889. [CrossRef]

13. Suwal, N.; Huang, X.; Kuriqi, A.; Chen, Y.; Pandey, K.P.; Bhattarai, K.P. Optimisation of cascade reservoir operation considering environmental flows for different environmental management classes. *Renew. Energy* **2020**, *158*, 453–464. [CrossRef]
14. Guimarães, S.O.; Costa, A.A.; Vasconcelos, F.d.C., Jr.; da Silva, E.M.; Sales, D.C.; de Araújo, L.M., Jr.; de Souza, S.G. Projeções de mudanças climáticas sobre o nordeste Brasileiro dos modelos do CMIP5 e do CORDEX. *Rev. Bras. Meteorol.* **2016**, *31*, 337–365. [CrossRef]
15. Marengo, J.A.; Alves, L.M.; Alvala, R.C.S.; Cunha, A.P.; Brito, S.; Moraes, O.L.L. Climatic characteristics of the 2010-2016 drought in the semiarid northeast Brazil region. *An. Acad. Bras. Cienc.* **2018**, *90*, 1973–1985. [CrossRef] [PubMed]
16. Silveira, C.d.S.; Filho, F.d.A.d.S.; Costa, A.A.; Cabral, S.L. Performance assessment of CMIP5 models concerning the representation of precipitation variation patterns in the twentieth century on the northeast of Brazil, Amazon and Prata Basin and analysis of projections for the scenery RCP8.5. *Rev. Bras. de Meteorol.* **2013**, *28*, 317–330. [CrossRef]
17. Silveira, C.D.S.; Souza Filho, F.D.A.D.; Martins, E.S.P.R.; Oliveira, J.L.; Costa, A.C.; Nobrega, M.T.; Souza, S.A.D.; Silva, R.F.V. Mudanças climáticas na bacia do rio São Francisco: Uma análise para precipitação e temperatura. *Rev. Bras. Recur. Hidricos* **2016**, *21*, 416–428. [CrossRef]
18. Fernandes, R.D.O.; Silveira, C.D.S.; Studart, T.M.D.C.; Souza Filho, F.D.A.D. Reservoir yield intercomparison of large dams in Jaguaribe Basin-CE in climate change scenarios. *RBRH* **2017**, *22*. [CrossRef]
19. Silva, M.V.M.D.; Silveira, C.D.S.; Silva, G.K.D.; Pedrosa, W.H.D.V.; Marcos, A.D., Jr.; Souza Filho, F.D.A. Projections of climate change in streamflow and affluent natural energy in tbrazilian hydroelectric sector of cordex models. *Rev. Bras. Recur. Hidricos* **2020**, *25*, 1–15. [CrossRef]
20. Eyring, V.; Bony, S.; Meehl, G.A.; Senior, C.A.; Stevens, B.; Stouffer, R.J.; Taylor, K.E. Overview of the Coupled Model Intercomparison Project Phase 6 (CMIP6) experimental design and organization. *Geosci. Model Dev.* **2016**, *9*, 1937–1958. [CrossRef]
21. O'Neill, B.C.; Tebaldi, C.; Van Vuuren, D.P.; Eyring, V.; Friedlingstein, P.; Hurtt, G.; Knutti, R.; Kriegler, E.; Lamarque, J.F.; Lowe, J.; et al. The Scenario Model Intercomparison Project (ScenarioMIP) for CMIP6. *Geosci. Model Dev.* **2016**, *9*, 3461–3482. [CrossRef]
22. Thiessen, A.H. DISTRICT No. 10, GREAT BASIN. *Mon. Weather Rev.* **1910**, *38*, 786–791. [CrossRef]
23. Barros, F.V.F.; Alves, C.d.M.; Martins, E.S.P.R.; Reis, D.S., Jr. The development and application of Information System for Water Management and Allocation (SIGA) to a negotiable water allocation process in Brazil. *J. Chem. Inf. Model.* **2013**, *53*, 1689–1699.
24. ANA. *Conjuntura Dos Recursos Do Brasil*; ANA: Brasília, Brazil, 2017; Volume 169.
25. CHESF Companhia Hidro Elétrica de São Francisco (Chesf). Available online: https://www.chesf.gov.br/SistemaChesf/Pages/SistemaGeracao/Sobradinho.aspx (accessed on 10 February 2020).
26. ANA. Hidroweb. Available online: http://www.snirh.gov.br/hidroweb/apresentacao (accessed on 10 September 2020).
27. Harris, I.; Osborn, T.J.; Jones, P.; Lister, D. Version 4 of the CRU TS monthly high-resolution gridded multivariate climate dataset. *Sci. Data* **2020**, *7*, 1–18. [CrossRef]
28. Cemig Usina Hidrelétrica de Três Marias. Available online: https://novoportal.cemig.com.br/usina/tres-marias/ (accessed on 20 February 2020).
29. Swart, N.C.; Cole, J.N.S.; Kharin, V.V.; Lazare, M.; Scinocca, J.F.; Gillett, N.P.; Anstey, J.; Arora, V.; Christian, J.R.; Hanna, S.; et al. The Canadian Earth System Model version 5 (CanESM5.0.3). *Geosci. Model Dev.* **2019**, *12*, 4823–4873. [CrossRef]
30. Boucher, O.; Servonnat, J.; Albright, A.L.; Aumont, O.; Balkanski, Y.; Bastrikov, V.; Bekki, S.; Bonnet, R.; Bony, S.; Bopp, L.; et al. Presentation and Evaluation of the IPSL-CM6A-LR Climate Model. *J. Adv. Model. Earth Syst.* **2020**, *12*, 1–52. [CrossRef]
31. Hirota, N.; Ogura, T.; Tatebe, H.; Shiogama, H.; Kimoto, M.; Watanabe, M. Roles of shallow convective moistening in the eastward propagation of the MJO in MIROC6. *J. Clim.* **2018**, *31*, 3033–3047. [CrossRef]
32. Wu, T.; Lu, Y.; Fang, Y.; Xin, X.; Li, L.; Li, W.; Jie, W.; Zhang, J.; Liu, Y.; Zhang, L.; et al. The Beijing Climate Center Climate System Model (BCC-CSM): The main progress from CMIP5 to CMIP6. *Geosci. Model Dev.* **2019**, *12*, 1573–1600. [CrossRef]
33. Yukimoto, S.; Kawai, H.; Koshiro, T.; Oshima, N.; Yoshida, K.; Urakawa, S.; Tsujino, H.; Deushi, M.; Tanaka, T.; Hosaka, M.; et al. The meteorological research institute Earth system model version 2.0, MRI-ESM2.0: Description and basic evaluation of the physical component. *J. Meteorol. Soc. Japan* **2019**, *97*, 931–965. [CrossRef]
34. Kriegler, E.; Bauer, N.; Popp, A.; Humpenöder, F.; Leimbach, M.; Strefler, J.; Baumstark, L.; Bodirsky, B.L.; Hilaire, J.; Klein, D.; et al. Fossil-fueled development (SSP5): An energy and resource intensive scenario for the 21st century. *Glob. Environ. Chang.* **2017**, *42*, 297–315. [CrossRef]
35. Fujimori, S.; Hasegawa, T.; Masui, T.; Takahashi, K.; Herran, D.S.; Dai, H.; Hijioka, Y.; Kainuma, M. SSP3: AIM implementation of Shared Socioeconomic Pathways. *Glob. Environ. Chang.* **2017**, *42*, 268–283. [CrossRef]
36. Fricko, O.; Havlik, P.; Rogelj, J.; Klimont, Z.; Gusti, M.; Johnson, N.; Kolp, P.; Strubegger, M.; Valin, H.; Amann, M.; et al. The marker quantification of the Shared Socioeconomic Pathway 2: A middle-of-the-road scenario for the 21st century. *Glob. Environ. Chang.* **2017**, *42*, 251–267. [CrossRef]
37. Riahi, K.; van Vuuren, D.P.; Kriegler, E.; Edmonds, J.; O'Neill, B.C.; Fujimori, S.; Bauer, N.; Calvin, K.; Dellink, R.; Fricko, O.; et al. The Shared Socioeconomic Pathways and their energy, land use, and greenhouse gas emissions implications: An overview. *Glob. Environ. Chang.* **2017**, *42*, 153–168. [CrossRef]
38. Hargreaves, B.G.H. Reference evapotranspiration By George, H. Hargreaves, 1 Fellow, ASCE. *J. Irrig. Drain. Eng.* **1994**, *120*, 1132–1139. [CrossRef]
39. Hargreaves, G.H.; Samani, Z.A. Relation between curve number and runoff coefficient. *J. Irrig. Drain. Eng.* **1983**, *109*, 240.

40. Feola, G. What (science for) adaptation to climate change in Colombian agriculture? A commentary on "A way forward on adaptation to climate change in Colombian agriculture: Perspectives towards 2050" by J. Ramirez-Villegas, M.; Salazar, A.; Jarvis, C.E. Navarro-Valc. *Clim. Change* **2013**, *119*, 565–574. [CrossRef]
41. Silveira, C.D.S.; Vasconcelos Junior, F.D.C.; Souza Filho, F.D.A.D.; Guimarães, S.O.; Marcos, A.D., Jr.; Dos Reis, G.N.L.; Porto, V.C. Performance evaluation of AR5-CMIP5 models for the representation of seasonal and multi-annual variability of precipitation in Brazilian hydropower sector basins under RCP8.5 scenario. *Hydrol. Sci. J.* **2019**, *64*, 1279–1296. [CrossRef]
42. Fang, G.H.; Yang, J.; Chen, Y.N.; Zammit, C. Comparing bias correction methods in downscaling meteorological variables for a hydrologic impact study in an arid area in China. *Hydrol. Earth Syst. Sci.* **2015**, *19*, 2547–2559. [CrossRef]
43. Lopes, J.E.G.; Braga, B.P.F.; Canejo, J.G. SMAP—A Simplifi ed Hydrological Model, Applied Modelling in Catchment Hydrology. *Water Resourses Publ.* **1982**, *1*, 1982.
44. Andrade, C.W.A.; Montenegro, S.M.G.L.; Lima, J.R.S.; Montenegro, A.A.A.; Magalhães, A.G. Modelagem hidrológica sob escassez de dados na Bacia do Alto Mundaú, Nordeste do Brasil. *J. Environ. Anal. Prog.* **2017**, *1*, 36–43. [CrossRef]
45. Nash, E.; Sutcliffe, V. River Flow Forecasting Though Conceptual Models Part I- A Discussion of Principles. *J. Hydrol.* **1970**, *10*, 282–290. [CrossRef]
46. Lima, J.P.R.; Alves, J.M.B. Um Estudo de Downscaling Dinâmico de precipitação Intrasazonal Acoplado a Modelo Chuva-vazão na Bacia Hidrográfica Alto-médio São Francisco. *Rev. Bras. Meteorol.* **2009**, *24*, 323–338. [CrossRef]
47. ANA. *Manual dos Usos Consuntivos de Água do Brasil*; Soares, S.R.A., Fontenelle, T.H., Garcia, C.S., da Cunha, L.M., Eds.; ANA: Brasília, Brazil, 2019; ISBN 9788582100578.
48. Brown, R.G. Statistical Forecasting for Inventory Control. *Davies J. R. Stat. Soc. Ser. A* **1960**, *123*, 348–349.
49. Holt, C.C. Forecasting seasonals and trends by exponentially weighted moving averages. *Int. J. Forecast.* **1957**, *20*, 5–10. [CrossRef]
50. Winters, P.R. Forecasting Sales by Exponentially Weighted Moving Averages. *Manag. Sci.* **1960**, *6*, 231–362. [CrossRef]
51. Hyndman, R.J.; Koehler, A.B.; Snyder, R.D.; Grose, S. A state space framework for automatic forecasting using. *Int. J. Forecast.* **2002**, *18*, 439–454. [CrossRef]
52. Gardner, E.S. Exponential smoothing: The state of the art-Part II. *Int. J. Forecast.* **2006**, *22*, 637–666. [CrossRef]
53. Hyndman, R.J.; Akram, M.; Archibald, B.C. The admissible parameter space for exponential smoothing models. *Ann. Inst. Stat. Math.* **2008**, *60*, 407–426. [CrossRef]
54. Taylor, W. James Exponential smoothing with a damped multiplicative trend. *Int. J. Forecast.* **2003**, *19*, 715–725. [CrossRef]
55. Brandão, J.L.B. Modelo Para Operação de Sistemas de Reservatórios Com Usos Múltiplos. Ph.D. Thesis, University of São Paulo, São Paulo, Brazil, July 2004; p. 182.
56. Brighenti, T.M.; Bonumá, N.B.; Chaffe, P.L.B. Calibração hierárquica do modelo swat em uma bacia hidrográfica catarinense. *Rev. Bras. Recur. Hidricos* **2016**, *21*, 53–64. [CrossRef]
57. Moreira, J.G.D.V.; Naghettini, M. Detecção de Tendências Monotônicas Temporais e Relação com Erros dos Tipos I e II: Estudo de Caso em Séries de Precipitações Diárias Máximas Anuais do Estado do Acre. *Rev. Bras. Meteorol.* **2016**, *31*, 394–402. [CrossRef]
58. Yue, S.; Cavadias, G. Power of the Mann ± Kendall and Spearman's rho tests for detecting monotonic trends in hydrological series. *J. Hydrol.* **2002**, *259*, 254–271.
59. Collischonn, W.; Dornelles, F. *Hidrologia Para Engenharia e Ciências Ambientais*; ABRH: Porto Alegre, Brazil, 2013.
60. Knight, J.R.; Folland, C.K.; Scaife, A.A. Climate impacts of the Atlantic multidecadal oscillation. *Geophys. Res. Lett.* **2006**, *33*, 2–5. [CrossRef]
61. Trenberth, K.E.; Cheng, L.; Jacobs, P.; Zhang, Y.; Fasullo, J. Hurricane Harvey Links to Ocean Heat Content and Climate Change Adaptation. *Earth's Futur.* **2018**, *6*, 730–744. [CrossRef]
62. De Jong, P.; Kiperstok, A.; Torres, E.A. Economic and environmental analysis of electricity generation technologies in Brazil. *Renew. Sustain. Energy Rev.* **2015**, *52*, 725–739. [CrossRef]